Politecnico di Torino

Energy and Nuclear Engineering

Sustainable Nuclear Engineering

Master's Thesis

Joining of SiC/SiC composite materials through preceramic polymers for nuclear fuel claddings

Professor:
Ferraris Monica

Student:
Tresso Marco

November 2024

Acknowledgments

This thesis was made possible thanks to the GLANCE group in the DISAT department and the J-Tech@PoliTo laboratory, which warmly welcomed me into their spaces.

I am deeply grateful to Professor Monica Ferraris for her guidance and support throughout these months of work. I also want to thank Aurora Pizzinat, who kindly taught me the procedures and techniques I needed to complete this thesis, and Daniele D'Ambrosio, whose help in the laboratory and daily encouragement were essential—none of this would have been possible without him.

Abstract

This thesis explores the use of Ceramic Matrix Composites (CMCs), specifically silicon carbide (SiC/SiC), for applications in high-stress environments such as nuclear energy. The research focuses on an experimental approach to joining silicon carbide composite components using preceramic polymers, specifically polycarbosilanes, as a binding material. These polymers undergo a transformation from polymer to ceramic during a thermal process, including pyrolysis at temperatures up to 1500°C. Challenges associated with this method include material shrinkage during pyrolysis, porosity, and interface wettability, all of which impact the joint integrity. These challenges are addressed within the framework of the study, which aims to expand the functionality of advanced ceramics in complex geometries, thus enhancing their industrial applicability. By demonstrating the feasibility of such techniques for nuclear-grade components, this work contributes to the broader understanding of advanced ceramic applications in high-stress fields, promoting enhanced safety and efficiency. The findings are presented across five chapters, covering theoretical background, preceramic polymer properties, experimental procedures, results, and future implications.

Contents

Chapter 1

Introduction

Nuclear engineering is often strictly related to materials engineering when it comes to feasibility studies concerning temperature resistance, corrosion resistance, airtightness, irradiation behavior and so on.

Ceramic Matrix Composites (CMC) materials are recently growing in researches to be used in aggressive environments, such as aeroengines and correlated objects or nuclear energy production, as well as heat exchangers, all fields in which severe mechanical, structural and thermal stresses are engineering factors to take into account in the design and construction of the components of the said activities.

1.1 Purposes of the thesis

The present thesis is an experimental work and the precise purpose will be clear in the next chapters with the deep explanation of the state of art and theoretical background.

The aim is to join two elements of silicon carbide composites by using as joining material a polymeric precursor of ceramics able to change its state of polymer to a state of ceramic undergoing a thermal process that includes pyrolisis and temperatures up to 1500°C.

The challenge concerns the use of a technology not widely used yet for joints but rather for 3D printing and different applications. Preceramic polymers applied to this work's purpose face some issues to be solved, such as the shrinking of the material during pyrolisis, the remaining porosity, the wettability at the interfaces and others that will be studied in detail.

The utility of the research lays on the concrete possibility of easily creating complex geometries for a ceramic, that is a goal that would permit a wider use of ceramics in the industrial sector. The use of ceramics in small and simple geometries has always been a limit of this materials' family, but actually advanced ceramics have unique features that could help in building components of tools in aerospace engineering and in applications in the field of energy thanks to their strong thermal and mechanical intrinsic resistances.

When speaking about *nuclear grade* components, it is meant a piece that meets the strict quality, safety, and reliability standards required for use in nuclear power plants or other nuclear-related applications. In chapter 1.4 it is well explained how SiC/SiC can be a nuclear grade material and can enhance the current technologies in fission light water nuclear reactors (LWR).

Chapter one is the introduction and presents a theoretical background on ceramics and the materials that are going to be used in the experimental activity.

Chapter two presents a study on preceramic polymers going into explaining the specifics of the polymer that is going to be used and the ways to solve the problems related to it.

Chapter three explains the steps and the instruments used in the experimental activity. It is the core of the work together with chapter four.

Chapter four presents the results of the thesis and a critical theoretical justification of them.

Chapter five concludes the work and presents the possible future perspectives summing up the state of art successive to the present work.

1.2 The European projects "Il Trovatore" and "Scorpion"

The 2011 Fukushima Daichii event demonstrated the need for safer nuclear energy, which can be achieved by developing accident-tolerant fuels (ATFs). ATFs are expected to overcome the technical shortcomings of the standard zircaloy/UO_2 fuels, thus relieving the industry from the financial penalty associated with severe accidents causing fuel cladding failure and release of radioactive fission products to the power plant containment & environment.

The main IL TROVATORE objective is to identify promising candidate ATF cladding materials for use in Gen-II/III LWRs and validate them in industrially-relevant conditions, i.e. via neutron irradiation in PWR-like water. The innovative ATF clads should demonstrate significant improvement in performance compared to standard fuel clads (zircaloys), thus taking a step towards safer nuclear energy worldwide.

ATF clads must outperform commercial zircaloy clads by satisfying two requirements: (a) achieve a step enhancement in performance during nominal operation conditions & short-lived design-basis transients (<1200°C), and (b) maintain hermeticity for prolonged periods during beyond-design-basis accidents (>1200°C).

The ATF cladding material concepts studied in the project are:

- SiC/SiC composite clads: various processing routes, microstructures & performances (mid-term technology)
- Coated clads: protective coatings on zircaloy substrates; innovative coatings: (a) MAX phases, and (b) doped oxides; industrial coating: chromium (Cr) (near-term technology)
- GESA surface-alloyed clads: the surface modification of clads aims at the in-service formation of protective oxide scales. The GESA process modifies the surface of clads by means of an intense pulsed electron beam; the depth of the modification is limited, thus not affecting the bulk clad properties (near-term technology)
- Oxide-dispersed-strengthened (ODS) FeCrAl alloy clads: these alloys combine the high-T oxidation resistance of FeCrAl alloys with the resistance of ODS ferritic alloys to irradiation creep and swelling (mid-term technology)

The successful development of ATF clads will make the carbon-free nuclear energy safer, protecting society & environment; eliminate redundant safety systems in current reactor designs, improving their market profile; and strengthen the competitiveness of European industries in nuclear and non-nuclear sectors.

IL TROVATORE is an international collaboration (Europe, USA, Japan) combining academic excellence with industrial support, involving standardization bodies and nuclear safety regulatory authorities to accelerate the transfer of material innovation to market.

Part of the main materials used in this experimental activity were supplied thanks to this project, particularly the composite silicon carbide in these two shapes:

1. Slabs were the substrates are extracted, showed in figure 3.1
2. Cylinders and caps for the clad-like joining

SCORPION is an international collaborative project involving 16 partners from the EU, the UK, the USA, Japan, and Switzerland, and focusing on innovative ATF cladding materials.

The post-Fukushima global investments in ATFs (both fuels & fuel cladding materials) expect to overcome the inherent technical shortcomings of the standard zircaloy claddings/UO2 fuels currently used in Gen-II/III light water reactors (LWRs).

The timely deployment of ATFs will not only relieve the industry from financial penalties associated with beyond-design-basis accidents, but also protect society and environment from the adverse consequences of such events.

SCORPION focuses on the radical performance optimization of the SiC/SiC composite ATF cladding material concept, which is considered a 'revolutionary' concept as compared to the 'evolutionary' Cr-coated zircaloy ATF cladding material concept soon to be deployed.

The intended in SCORPION performance optimization of SiC/SiC composite ATF claddings targets primarily their inadequate compatibility with the coolant (water/steam) and the early (<2 dpa) saturation of radiation-induced swelling during nominal operation.

1.3 Recall on Advanced Ceramics

Broadly speaking, ceramic materials are nonmetallic, inorganic materials, that is, not metals, not plastics, not organic chemicals. They are materials used and appreciated for their characteristically high melting point, low thermal expansion, and good chemical resistance. These features are due to a combination of ionic and covalent bonds in the latter, in which the ionic predominates and create a strong electrostatic attraction between atoms. [1]

On the other hand, ceramics have also some undesirable characteristics, such as brittleness, that leads to fracture under certain conditions. The issue can be solved or at least reduced in intensity in different ways, including the formation of composite materials, that are heterogeneous materials composed of two or more integrated constituents.

They are made by different techniques depending on the use: particularly, the added constituent can be made of particulates (Oxide Dispersion Strengthen materials are an example, used in claddings for their creep resistance and low ductility), whiskers, and finally fibers.

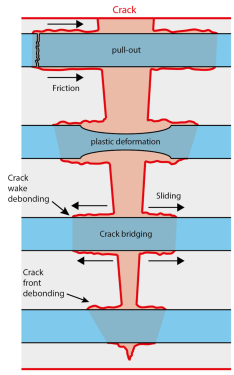

Figure 1.1: Crack energy dissipation [2]

Regarding ceramics, fibers reinforced materials are a very effective way of reducing the brittleness intrinsic of the material. In this class, (Ceramic Matrix Composite) materials are widely studied: they are composite in which the matrix and the fibers are both ceramics, often the exact same material. The presence of the fibers stop the propagation of cracks by absorbing the energy with the fiber pull-out caused by the crack defection due to the weak interface between the matrix and the reinforcement as shown in figure 1.1, so that the material takes a quasi-ductility behavior and reduces drastically the brittleness. [2]

Thanks to these unique features, in the last 60 years the use of composite materials has grown substituting metal alloys in many fields (figure 1.2), especially in aerospace high-tech engineering for mechanical and thermal properties, biomedical application for electrical and resistance ones, and energy in the nuclear field in which they are used already as for example core catcher material

for thermal properties and it's currently studied to extend the application to the cladding of fuel pins and other areas of particular stress inside of the reactor.

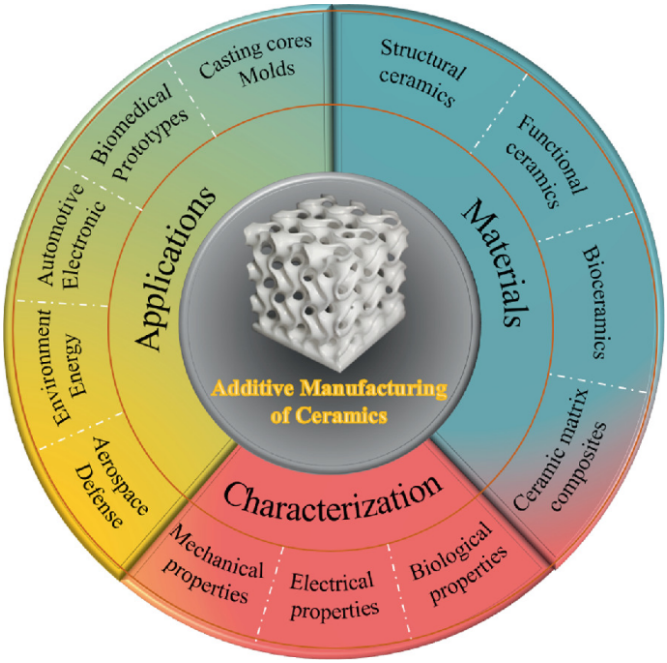

Figure 1.2: Advanced Ceramics uses [3]

1.4 Silicon Carbide as an ATF material in Light Water Reactors

The main challenge in the use of ceramic materials is to build big and complex components, because they do not melt (or at very high temperatures) and their brittle behavior makes their mechanical shaping quite challenging. Furthermore, ceramics have properties strongly size-dependent following the Weibull's distribution, that defines how the probability of finding a critical defect inside a ceramic component arises with the size of the component itself.

The aim of the experimental activity is then finding efficient techniques of joining simple pieces of ceramics in order to have as a result a more complex geometry. It is particularly difficult to bond SiC/SiC composites via direct joining techniques. SiC melts incongruently at around 2700 °C, a temperature at which it transforms from a monophasic solid to a biphasic system of liquid and carbon. In such a case, welding is not possible. [4]

In nuclear R&D the focus is on the Accident Tolerant Fuel (ATF) materials, that are supposed to be used as the set of the UO_2 pellets and the cladding composing the fuel rod. Even if the current technologies applied to fission reactors guarantee a high quality and a safe working environment, enhancements can be made and in this document a ceramic alternative to "Zircaloy", that is the alloy currently used as the cladding of LWR's fuel rods, is studied with a focus on the joining of the composite material SiC_f/SiC through preceramic polymers. [5]

Zircaloy has been developed and used for its excellent properties suitable for the role, for example the low cross section for absorption of thermal neutrons (0.22 barns according to Allegheny Technologies Incorporated technical sheet), the adequate strength and ductility the compatibility with the fuel and the corrosion resistance to water, together with the high melting T (1845°C). Its composition is of about 95% Zr, 1.5% Sn, 0.2% Fe, 0.1% Cr. Zirconium alloys have superior thermal properties compared to other traditional materials in consideration for spent nuclear fuel containers. Zirconium alloys have a thermal conductivity more than 30% higher than stainless

steel alloys. The linear coefficient of thermal expansion for Zirconium alloys is nearly one-third the value for stainless steel giving Zirconium alloys superior dimensional stability at elevated temperatures. This is an advantage also in nuclear waste containers where temperatures could exceed 200^{o}C for hundreds of years.[5]

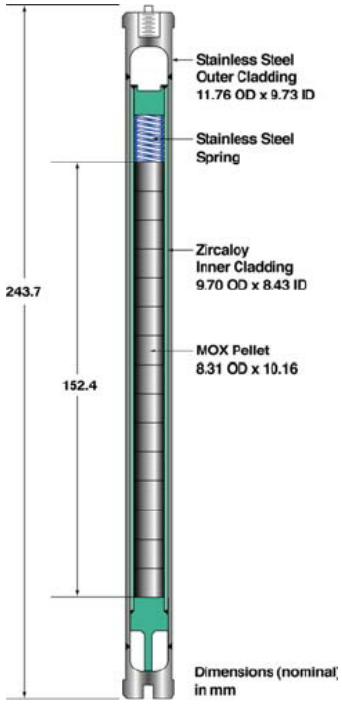

Figure 1.3: Example of current typical fuel pin in LWRs

The willingness to substitute the Zirconium alloy is due to some disadvantages of the material. As a matter of fact, Zirconium used as clad is much more likely to permit the escape of fission release gases into the gap and plenum with respect to SiC, together with the fact that Zirconium undergoes a strong oxidation if reacting with water at high temperatures, as clear in figure 1.4 showing that Zirconium has a significantly higher oxidation rate constant with respect to most of the materials, including SiC.

The problem that makes it a non-ATF material is that the oxidation rate of Zircaloy in presence of high temperature steam causes a production of molecular hydrogen, following the reaction

$$2H_2O + Zr \rightarrow ZrO_2 + 4H_2 \tag{1.1}$$

that is an esothermic reaction, that implies a risk of explosion.[6]

This reaction was responsible for explosions in the accidents of Three Miles Island in 1979 and later in the Fukushima Daiichi one in 2011, as well as in the famous Chernobyl accident in 1986 but successively to the steam leakage. [5]

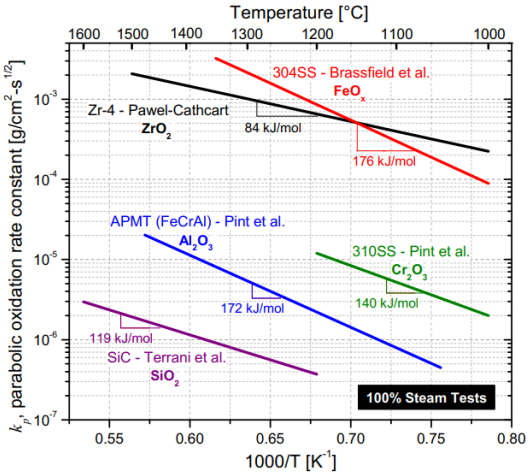

Figure 1.4: Zircaloy disadvantages

On the other hand, composite materials, specifically SiC/SiC are being studied and improved nowadays at fast pace due to their high performance in structures at high temperature. SiC_f/SiC shows high strength, high stiffness, low density, and high thermal and chemical stability to withstand long exposures at elevated temperatures. Silicon carbide, together with other composite materials such as FeCrAl and ODS (Oxide Dispersion Strengthened), is then of the more promising alternatives to Zircaloy, that is also for prevent LOCAs (Loss Of Coolant Accidents), that are severe accidents hardly manageable in a nuclear reactor consisting of the reduced presence of coolant (water in LWR).

The rod containing uranium dioxide pellets would not be composed exclusively of CMC, but in order to be considered an ATF for LWR, it is conceived as a three layers cylinder as in figure 1.5, with the inner and outer layers made of monolithic SiC obtained through CVD (Chemical Vapour Deposition) and the internal layer of SiCf/SiC, with the thickness shown in the figure 1.5.

The SiCf/SiC layer is responsible for the mechanical resistance (see paragraph 1.1) in case of accident, while the two remaining layers work as barriers: the inner layer is at direct contact with the nuclear fuel, so it contains the fission releases gases, while the outer one is a barrier in terms of water corrosion, that by the way is typically at high T (about 330-350°C for LWRs).

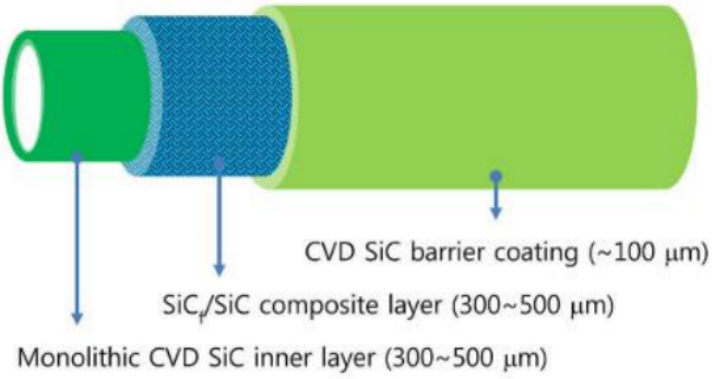

Figure 1.5: Schematic composition of Triplex [7]

It is important to specify that LWRs are not the only possible application of SiC/SiC in nuclear environment: SiCf/SiC is an attractive material also for nuclear fusion engineering, and it has

been considered in several power plant studies, such as the TAURO, DREAM, and ARIES-AT design studies. The interest concerns the very high temperature resistance, together with all the mechanical properties already mentioned, but above all the exceptionally low activation under 14-MeV neutron radiation. [8]

1.4.1 Silicon carbide properties on neutron radiation

SiC is a material considered under the due conditions, an ATF because of the respect of the nuclear parameters, but it faces some issues when irradiated with neutrons.

Specifically, a relevant phenomenon is the volumetric swelling, that is strongly dependent on the temperature but almost not at all on the dpa, so the dose range, as in figure 1.6 is well shown.

With the addition of fibers (see paragraph 2.4), the swelling does not change significantly: in figure 1.6 the case material is CVD SiC reinforced with fibers from the japanese company Hi-Nicalon™.[9]

The most drastic change in size was measured at the lowest temperature (300°C), reported also by Perez-Bergquist et al. [10] with SiC/SiC with an interface of PyC (Pyrolitic Carbon), which was subjected to high dose of neutrons to levels >70 dpa. In that case the most influenced zone was the PyC interface, while small but relevant size changes were depicted in the silicon carbide matrix and the Hi-Nicalon™ fibers.

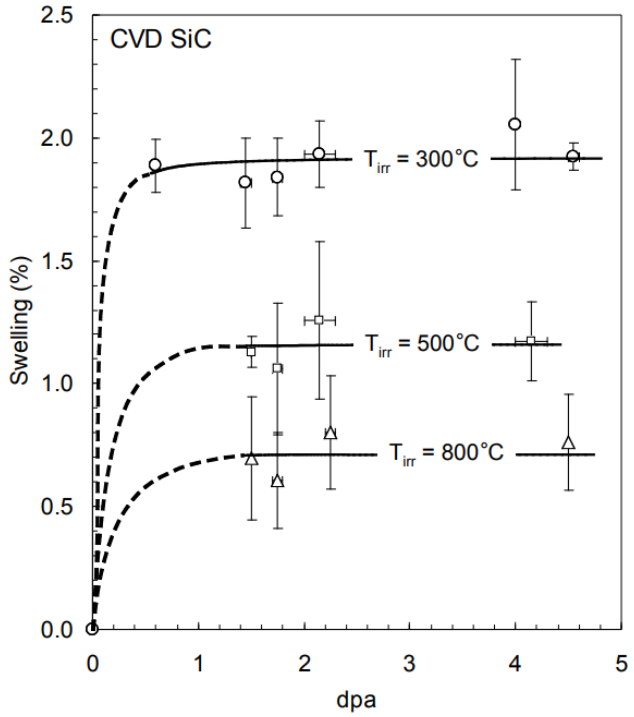

Figure 1.6: Effect of irradiation fluence and temperature on volume change of composites reinforced with Hi-Nicalon™ fibers [9]

Neutron irradiation influences the material performances even concerning the mechanical behavior. Particularly, it enhances the flexure strength of CVD silicon carbide, with the effect being temperature-dependent and saturating at relatively low fluence levels. However, irradiation reduces the variability in flexure strength across a large sample population, as indicated by a decrease in the Weibull modulus, which is also temperature-dependent. The specific flaws responsible for this change in strength and variability in irradiated CVD SiC are not yet understood. [9]

1.5 Joining techniques

The possible ways to join two materials are numerous and are chosen base on the type of material and use of the joint. They can be classified on different criteria, and one possible way is to distinguish mechanical, direct and indirect joints.

A mechanical joint is definitely not useful to the purpose of this thesis because it concerns screw joints and mechanical sealing systems that are not at all airtight and above all they are not homogeneous in the stress distribution, causing points of particular fracture risk. The whole point is indeed to avoid stress peaks inside of the joining region.

A direct joint does not use external materials and so it is a process applied only to the two joining components. The most obvious example is welding, that is a technique widely used in industrial processes, but with ceramics, especially with silicon carbide, this is impossible because SiC melts incongruently at around 2700 °C [11], a temperature at which it transforms from a monophasic solid to a biphasic system of liquid and carbon. [4]

Other direct joints can be used for ceramics such as diffusion bonding, but generally they are hard to realize, or at least harder than indirect joining techniques.

Indirect joints are those that use a third material to join the components, such as adhesives, brazing materials, precursors, that represent our case study, glass ceramics such as Calcia-Alumina [12], and more types of indirect materials.

Specifically for composite silicon carbide, here are presented some possible ways to join the studied material, that is a fiber-composite advanced ceramic.

1.5.1 Brazing

Brazing is an indirect joining technique that uses a metallic alloy, called brazing alloy, which has a melting point lower than the one of the materials to be joined.

The temperature is increased until the brazing alloy is liquid and penetrates into the composite and creates a strong bonding interface. The result, as shown in figure 1.7, is a shrink in the joining area of the brazing material and a bond created in the inside of the substrate.

Something on which the focus must be maintained is that the coefficient of thermal expansion of the brazing alloy and SiC/SiC must be similar, because otherwise at the end of the process the stress would be high and lead eventually to the fracture of the joint.

Figure 1.7: Schematic process of brazing [13]

Ceramics can not be wet by conventional metals because of their incompatibility due to the high surface tension given by the ionic or covalent bond and to the atomic structures of the two families of materials. [14]

To have an adequate wettability, that corresponds to a wetting angle $<90°$, while conventional metallic alloys have an angle of $\approx 180°$, as clear in figure 1.8, where the conventional metal alloy almost do not wet at all the slab.

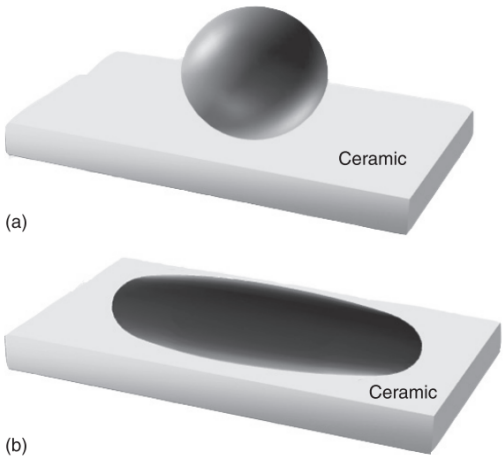

Figure 1.8: Wettability with conventional metals (a) and with active-brazing filler metal (b) [14]

To sum up, only certain types of metallic alloys can be used, typically pure Ti, Al-Ti, Cu-Ti, Si-Ti, Ag-Cu-Ti, Cu-Ag-Ti [15]. Other innovative alloys are being studied, specifically for SiC, like Zr-Cu as a filler metal as reported from Zhou et al. [16]

A special care has to be taken if applied to LWR fission reactors because in such case silver alloy must be avoided due to activation problems.[17]

A proposal for an optimized brazing alloy specifically designed for joining SiCf/SiC materials used in the nuclear sector comes from the "Commissariat à l'énergie atomique et aux énergies alternatives" (CEA) in France. These alloys, named BraSiC®, are non-reactive and primarily based on silicon, with small amounts of metals like Cr, V, Ti, Rh, etc. These metals are chosen to ensure the alloys have good wettability with SiCf/SiC composites, excellent resistance to high temperatures, and do not react with the CMC. For example, it has been shown that using the BraSiC® V3 alloy, after treatment at 1300°C in an inert atmosphere, results in a clean and homogeneous joint layer on SiCf/SiC.[8]

1.5.2 MAX phases

The name of these materials comes from the groups $M_{n+1}AX_n$, where n = 1, 2, or 3, M is an early transition metal (Sc, Ti, V, Cr, Mn, Fe, Co, Ni, Cu and Zn), A is an A-group element (specifically, the subset of elements 13–16), and X is carbon and/or nitrogen.

The compounds in this family share a specific structure, as shown in figure 1.9, consisting of overlapping hexagonal layers of tetrahedra and planes formed by the element from group A. The layers of element A are separated by n+1 layers of elements M. Within these compounds, the bonds exhibit a combination of covalent, ionic, and metallic character, with strong covalent M-X bonds within the layer where both are present, and relatively weaker M-A bonds. [18] [19]

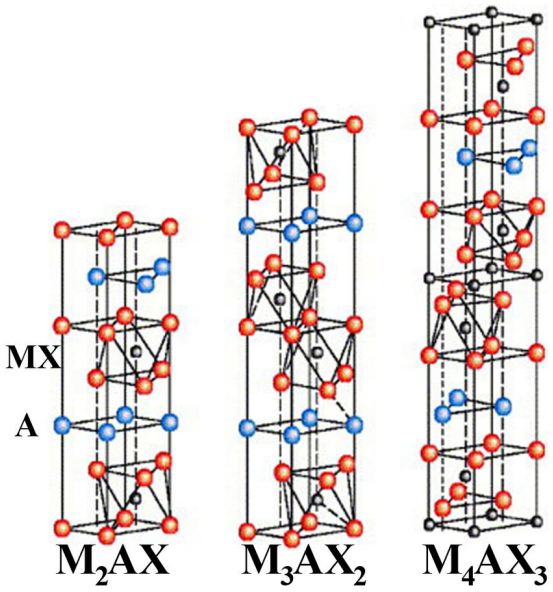

Figure 1.9: Max structure [19]

The mechanical behavior of MAX phases sets them apart from most conventional ceramics, like TiN or ZrC, as they are generally softer, with hardness levels around 2–8 GPa. This makes them less brittle and easier to machine. While they can exhibit pseudo-ductility at high temperatures due to the activation of basal slip systems, they usually revert to their brittle nature at lower temperatures. MAX phases are also known for their unique combination of metallic, covalent, and ionic bonding, stemming from the hybridization between the p and d orbitals of their constituent A and M atoms. This unique bonding gives them high electrochemical resistance, making them ideal for applications where corrosion resistance is crucial.

Another crucial feature of MAX phases is their refractory, since they assume the pseudo-ductility behavior over 1200°C, their fusion point is high (over 2000°C). On the other hand, oxidation resistance is not for granted: mainly, MAX phases oxidize as follows[18]:

$$M_{n+1}AX_n + bO_2 = (n+1)MO_{x/n+1} + AO_y + X_nO_{2b-x-y} \tag{1.2}$$

.

So, the oxidation resistance depends on the nature of the oxide.

The most resistant MAX phases compounds are the ones that can form a layer of Al_3O_2 that protects the exposed layer from oxygen, that are for example Ti_2AlC and Cr_2AlC. Generally, this materials' family is not useful in air right because of the oxidation issue.

Given their elastic behavior, nanolayered crystal structure, high corrosion resistance, and impressive high-temperature properties, MAX phases show potential for future applications in nuclear technology, particularly in high-temperature reactors. However, their use in irradiation environments requires further research to understand how exposure to energetic particle irradiation affects their crystal structure and how this damage develops and recovers within the material.[20]

So far, studies on their irradiation response have used two main methods: neutron irradiation in materials test reactors and ion irradiation via particle accelerators.

Considering that the dataset regarding neutron irradiation response of MAX phases is still poor, the most studied among these is Ti_3SiC_2, that has been studied specifically as a joining material for SiC/SiC, aimed to the structural application for LWR, because the irradiation experiments

are promising. It has been thought even to make big components composed entirely by Ti_3SiC_2, but the research on the joining technique is richer so far.

Specifically, Tunes et al.[20], conduced tests in which for the neutron irradiations, both bulk Ti-based MAX phases were irradiated at the ORNL's HFIR up to fluences of 2 × 1021 and 1 × 1022 n/cm^2. These fluences correspond to a dose of 2 and 10 dpa, respectively. The irradiations at the HFIR were carried out at a temperature of 1273 K.

Some irradiation effects within the microstructure of this material are clearly visible. For example, at 2 dpa, it is noticeable the presence of voids/cavities randomly distributed within the grain and with diameter of around 3–7 nm whereas. On increasing the dose to 10 dpa, long transgranular dislocation lines are observed to form within grains, and the formation of a disordered dislocation network is noted at the highest dose.[20]

Overall, the main concern in the structural use of these materials for industrial purposes such as Light Water Reactors, is the low oxidation resistance that in certain situations seems to be irrelevant but eventually it causes degradation in continuous severe conditions.[21]

1.5.3 Glass-ceramic phase

Among the proposed joining and coating methodologies for SiC/SiC composites, glass-ceramics have unique characteristics, such as softening at high temperatures and interesting properties. Moreover, glass-ceramics are not affected by oxidation, and can be self-sealant at temperatures above the glass softening point. If a single glass or glass-ceramic coating material cannot satisfy all the working conditions (i.e., thermal expansion coefficient, wettability, working temperature, sealing temperature, etc.), then the design of a double layer coating could be necessary.[22]

Glass-ceramics properties that are attractive for SiC/SiC joining are:

- Thermal expansion compatibility, that means that even at high temperatures the risk of crack for Δk (variation of the coefficient of thermal expansion) defined for the material, is reduced
- Good wetting behavior, essential for adhesion in the joint
- Controlled crystallization, for which the mechanical and thermal properties can be tailored based on the needed use
- High temperature resistance, as in they are thermally stable, shock resistant and they maintain a high quality at high temperatures
- Impermeability to gases

Literature about MAX phase materials is abundant and it often focuses on fusion application, specifically applied to the ceramic breeder Li_4SiO_4 that is one of the main candidates for tritium breeding in a Tokamak blanket. Ferraris et al.[12] tested Calcia-Alumina (CA) glass-ceramic on the said material and on SiC/SiC with a CVD SiC as matrix using a pressureless technique, concluding that it could be employed either as a joining or as a coating material.

Glass-ceramics can be treated both with laser to have a localized joining and in an oven during the thermal process. Considering the composition of the material and the conditions during the process, it is important to calculate and use the optimal sintering temperature, that averagely is between 1200°C and 1300°C.

There are doubts about the radiation resistance of glass-ceramics due to two competing processes: swelling and densification of the amorphous and crystalline phases. The main issue with these materials is assessing the shrinkage/swelling ratio and the differential volumetric changes between the various phases.

On the other hand, Calcia-Alumina and SAY (Silica-Alumina-Yttria), two glass-ceramics, have been tested under low and high dose irradiation in [23][24] and they resulted as suitable for

joining regarding neutron irradiation at temperatures in the order of 600-700°C of 20 dpa, as they did not undergo degradation despite swelling and densification phenomena.

1.5.4 Diffusion bonding

Diffusion bonding, also known as diffusion welding, is a solid-state joining process where two surfaces are bonded together through the diffusion of atoms at elevated temperatures and under pressure, without significant plastic deformation or the use of a filler material. The technique is typically used for joining similar or dissimilar metals and ceramics. It is an ideal process for materials that cannot be easily welded using traditional fusion methods such as SiC/SiC, which is our study-case.

A pure diffusion bonding joining would be ideal because the process would not involve any third material. In this case the technique assumes the name of *self diffusion bonding*. This process is attractive even from a perspective of *total SiC* joints, but unfortunately it has its limits: it is not at all pressureless, on the contrary it requires high pressures and temperatures for quite a long time up to 60 MPa and 2000°C for SiC, because also the temperature needs to be at least 75% of the welding temperature, that for SiC is 2700°C (actually it is not even a proper welding as explained in paragraph 1.4).[17]

The diffusion bonding without interlayer is possible thanks to the SPS (Spark Plasma Sintering) that prepare the surface (figure 1.10): the process requires a very high quality surface cleaning together with the high pressure and temperature.

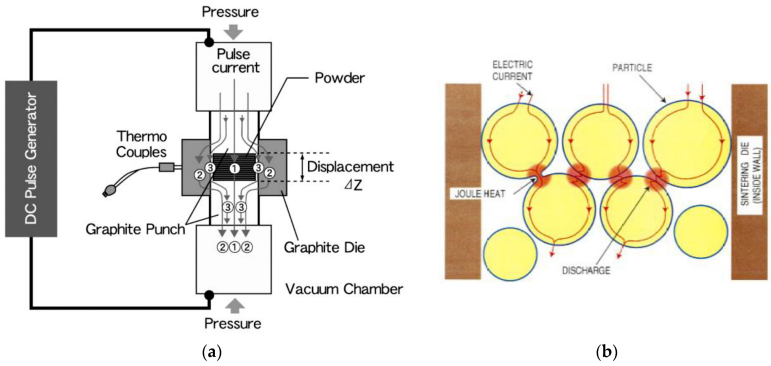

Figure 1.10: Diffusion Bonding process[25]

This is achieved, as shown in figure 1.10, by applying a electric field caused by a DC current impulse and a bidirectional pressure. The graphite in which the sample is settled is the conductive material to have the DC current useful.

The critical condition for diffusion bonding is the applied pressure, that must be precise. The technique was applied in experiments with Ti_3SiC_2, Au and even with SiC/SiC and C/SiC, but if the pressure is not perfectly optimized the result can turn out porous and dishomogeneous.[26]

1.5.5 Diffusion bonding with interlayer

There are times in which the technique of self diffusion bonding does not work, due to its complexity of conditions. A good alternative can be the use of an interlayer composed of a refractory material that diffuses well with the material and allows to produce a complete new phase and therefore a complete bond.

The most used material as third material is Titanium for its diffusivity and bonding properties. In the joining process for SiC, some problems arise, first in the list the formation of TiC, that is a composition with difficult properties in this field: a strong mismatch in CTE and other relevant mechanical properties.

The process is done through Spark Plasma Sintering, so a high current is applied to a graphite structure that indirectly heats the joining and makes the reaction happen.

Grasso et al.[27] led experiments on CVD SiC and a Titanium foil (150 micron) as interlayer material. The SPS and interlayer position during the process is shown in figure 1.11. In the experiment, which is the first documented experiment for flash joining for ceramics, the current intensity peak is of 370 A with a heating power of 2.2 kW. The result of the SPS was a 9600°C/min heating for 7 s and an apparent shear strength of 31.4 MPa was obtained, that is stronger than the strength of the composite itself.

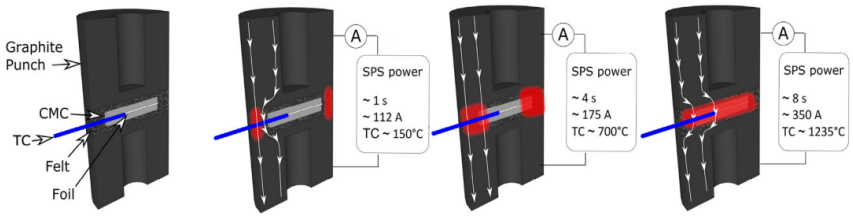

Figure 1.11: Process for diffusion bonding with Ti interlayer [27]

The process is then working and successful, but for nuclear application it cannot be used because of the formation of titanium carbide, as said.

The use of Titanium can bring to the formation of MAX phases, but another candidate material for interlayer is molybdenum that, with minimum joining temperatures of 1200°C, gave better result with 100% of the transformation of the phase, but still the CTE mismatch is intense, even if lower, so the nuclear application is, for now, not an used option, as it is usual for indirect joining using third materials. [15]

1.5.6 Polymeric precursor

The concept is to use a polymeric material, one of those presented in figure 2.1, that are special materials able to transform in a ceramic if submitted to thermal processes.

The process will then have as a result a ceramic without the step of sintering, but rather through cross-linking and pyrolisis, that can be achieved in different ways, such as in ovens.

The big promise gave from these materials is the fact that in the end, to join ceramics, there is not a third material and therefore the CTE and physical mismatch issue disappears. Clearly, the selected polymer must be leading at the end of the process to the substrate's material that in our case is silicon carbide, and so the correspondent precursor is polycarbosilane (section 2.1.2).

The problems related to this technology are, then, not about physical properties incompatibility, but rather about in-process changes that are consequent to the change of the lattice. That is, the polymer has an amorphous structure, and it is often a liquid, while the ceramic is solid and with a packed structure, crystalline and dense. With this premises, the problem is that during the formation of the ceramic, in the pyrolisis phase, the material is going to become much more dense and therefore reduce its volume, resulting in a porous joining or coating.

It is not only the volume that undergoes relevant changes. In fact, the polymer contains volatile compounds that burn in the oven and so also the mass decreases, and that is verifiable through a thermogravimetry as the one in De Vivo.[15]

To overcome the volumetric and mass issues fillers are used in shapes of whiskers, fibers or powder. For example, in our case study, adding fibers of SiC in a polycarbosilane ideally results in a SiC_f/SiC joining zone.

1.5.7 Refractory Metal Wrap

RM-Wrap technology falls within the category of brazing, as it involves using a metallic filler material to achieve a joint. The process consists of placing a layer of Refractory Metals (Mo, Nb, Ta, Zr) and a portion of metallic silicon between two substrates.

The proportions must be such that, after controlled heating, the two metals react, fully converting the refractory metal into various silicides, that are cearmic particles. The most studied of these materials is Molybdenum, that reacting with silicon gives $MoSi_2$. The resulting joint material is called a "wrap" due to its architecture, where a thin layer of silicon is sandwiched between two refractory metal layers. One metal layer is roughly the same size as the silicon, while the other is larger, allowing its edges to fold over the smaller layers, as shown in figure 1.12. This configuration helps form ceramic silicides without requiring excessively high temperatures and prevents silicon, which becomes very fluid at high heat, from escaping the joint area. The joint is created through a simple heat treatment in a conventional furnace, conducted at around 1450°C for a short time without applying pressure, in an inert atmosphere.[28]

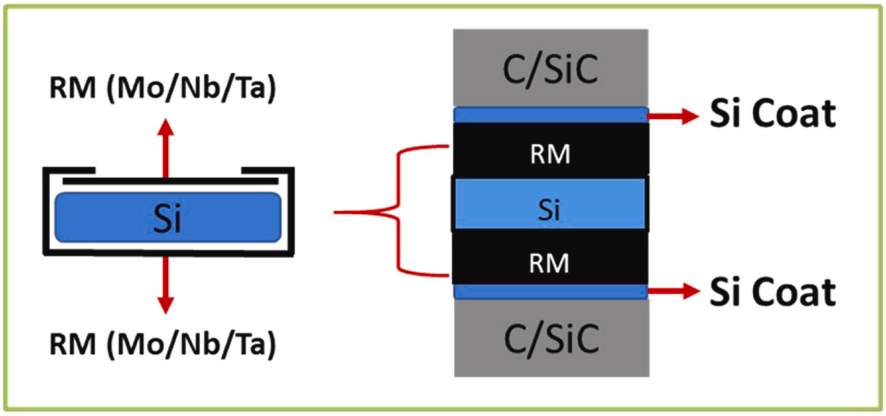

Figure 1.12: RM-Wrap technique configuration scheme [28]

In an ideal situation, the process should lead to a joining composed by Si and silicides. These lasts are very convenient especially in SiC_f/SiC joinings because they have a very similar CTE, in the range of 3.9-4.5x$10^{-6}K^{-1}$, and very good thermomechanical properties with melting point of around 2000°C. $MoSi_2$ is characterized by a CTE of 3.9x$10^{-6}K^{-1}$ [29].

In reality, the joining is not characterized by a perfect transformation in silicides, but the result is usually rather a composite material with particles of RM in a silicon matrix, because it is inevitable that some percentage of the silicon does not react, since it is given priority to the complete transformation of the RM to avoid metallic residues, that would be sensible to oxidation. Anyway, following studies can be aimed to optimize the Si/Mo ratio to improve the wettability of the composite.[15]

The mechanical properties of joints formed using refractory metal wraps are highly dependent on the processing parameters, including temperature, pressure, and bonding time. Research has shown that these joints can exhibit excellent shear and tensile strength, thanks to the RM layer absorbing and dissipating mechanical stresses.

1.5.8 Reaction forming bonding

This technique uses a filler material composed of silicon carbide (SiC) and carbon, with silicon infiltration heated slightly above its melting point (1414°C). The elevated temperature allows silicon to react with carbon, forming silicon carbide (SiC). As SiC forms, it expands, creating cracks within the material. Silicon, at the right viscosity, can infiltrate these cracks and react

with more carbon and so on until the cracks are all filled. The process occurs around 1450°C without the application of pressure.

The main advantage of this technique is that it ideally creates a joint layer with the same chemical composition as the substrates, ensuring good continuity of properties throughout the final product. However, this is an ideal goal, as residual free silicon is inevitably present in the joint layer, even when optimizing the composition of the filler mixture. The presence of both metallic silicon and SiC poses an intrinsic defect for materials intended for nuclear applications due to differential swelling between the two phases under neutron irradiation. Additionally, careful control of the process atmosphere is crucial: if the joint is made in the presence of air, silica would form, which, unlike SiC and pure metal, shrinks when exposed to neutron flux.

It is possible to optimize the initial filler material composition to reduce the amount of free silicon, although at least 10% remains. Studies suggest that segregating metallic silicon into small clusters, evenly distributed in the SiC matrix, may minimize issues arising from the differing mechanical behaviors of the two phases. [30]

Chapter 2

Preceramic polymers

In this thesis project, a special attention is given to obtaining a result that can withstand the nuclear grade environment, that is, high temperatures, strong gradients in temperature and pressure, high neutron irradiation resistance. A strongly desirable result that satisfies the high quality demand is to have a *Total SiC* piece in the end of the joining, that is preferable to a heterogeneous one to avoid drastically different behaviors at the interface that can lead to creep and eventually fracture.

Among all the joining techniques, the most suitable for the above-mentioned situation, is the use of preceramic polymers. They are mostly metallorganic compounds, usually based on silicon with additional elements, such as carbon, nitrogen, oxygen, or even metals, like boron or aluminium, in the backbone structure. [31]

In figure 2.1 it is described how Silicon bonded with different elements gives different kinds of polymers. Each one of the mentioned are able to get to ceramics if treated with the right process. Particularly, we are interested in obtaining Silicon Carbide ceramic, and that is possible through the cross-linking and the pyrolisis of polysilazanes (PSZ) and polycarbosilanes (PCS) polymers, that give high purity SiC: PSZ are transformed in SiC and Si_3N_4, while PCS in SiC and SiO_2. [32]

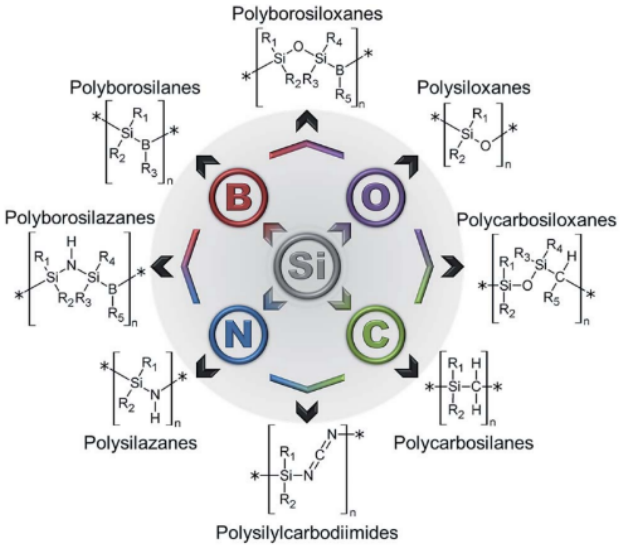

Figure 2.1: Examples of common families of Silicon-based polymers and their fundamental chemical units [31]

The research in preceramic polymers goes on since the early 1960s, when researchers like Ainger and Herbert, along with Chantrell and Popper, made a groundbreaking discovery by producing non-oxide ceramics from molecular precursors. About a decade later, Verbeek and his team took this a step further by demonstrating, for the first time, how polysilazanes, polysiloxanes, and polycarbosilanes could be transformed from polymers into ceramics. This process allowed them to create small-diameter Si_3N_4/SiC ceramic fibers designed for high-temperature applications. The field of polymer-derived ceramics (PDCs) saw significant advancements thanks to the work of Fritz and Raabe, as well as Yajima and his colleagues, who focused on synthesizing SiC ceramic materials through the thermolysis of polycarbosilanes. [33]

Traditionally, ceramics are prepared using powder technology, but this method has limitations, particularly due to the need for sintering additives, which can restrict technical applications. In contrast, the PDCs approach allows for the production of ceramic fibers, layers, or composite materials that are difficult or impossible to achieve using powder technology. Preceramic polymers offer versatility, as they can be processed or shaped through conventional polymer-forming techniques such as polymer infiltration pyrolysis (PIP), injection molding, coating from solvent, extrusion, or resin transfer molding (RTM). Once formed, these preceramic polymers can be converted into ceramic components by heating them to high temperatures, enabling the elements within the polymer structure to consolidate into a ceramic material.

The industry demand for this technology is wide, and it goes from Additive Manufacturing to 3D printing, including of course all the applications of joining studied in this thesis and in lots of other occasions.

The general process for preceramic polymers is thermal and happens through different steps:

1. The curing and the cross-linking are the first steps at the lowest temperature and they aim to chemically join the polymer chains through covalent bonds: in this stage of production, preceramic polymers undergo reactions that create a three-dimensional polymer network. These reactions, which occur below 200°C, incorporate functional groups like Si-H and Si-OH into the material's structure, transforming the precursors into thermosetting, non-meltable, and insoluble materials. [34]

   It is important that as a first material, there is a mixture of low molecular weight oligopolymers in order to optymize the volatility of organic material. This steps reduce in this way the mass of the system. The curing temperature can be possibly accelerated through catalysts.

2. The pyrolisis is a thermal decomposition process in which organic material is broken down into simpler chemical compounds by heating it in the absence (or near absence) of oxygen, so an oven with inert environment is necessary. This part of the process is critical because the phase composition, structure, and properties of the resulting amorphous ceramics are heavily influenced by it, along with factors like heating, reaction temperature, duration, and reaction atmosphere. Commonly used gases include argon or nitrogen, which help gradually remove gases emitted by the precursors. Oxygen and vacuum are used to form silicate ceramics and to promote crystallization through carbothermal reduction reactions. However, the chosen atmosphere will not react with any fillers that may have been added to the polymer. [35]

3. The last step that occurs at the highest temperature is the crystallization, that aims to compact the lattice and make the structure crystalline. The crystallization step typically occurs at temperatures between 1200-1800°C. [31] This transition from amorphous to crystalline happens because high temperatures cause the weaker chemical bonds in the amorphous ceramic material to break, leading to a rearrangement of functional groups. This process also results in the formation of some gaseous byproducts. The main factors influencing crystallization are the time and temperature of exposure, which specifically affect the development of crystalline nuclei within the material's structure.

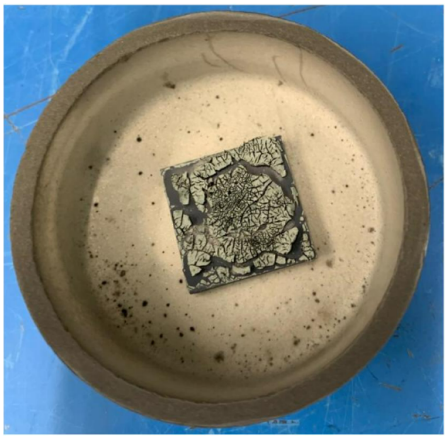

Figure 2.2: PCS after pyrolisis without additives[35]

A very valued advantage of using preceramic is that polymers can assume any desired shape, very useful feature in joining engineering. On the other hand, the main issue with this technique is that during the process the joining material undergoes a strong mass reduction, up to 50%, that makes the final product, if not properly treated, unsuitable concerning the presence of cracks and the high porosity that results.

Figure 2.2, from a previous thesis work ([35]), shows how the polymer looks like after the pyrolisis without additives, topic that is going to be deepened later, while in figure 2.3 the mass reduction trend is experimentally shown.

Generally, the mass and volumetric loss happens during the pyrolisis process and it is caused by the release of volatile compounds or light formation molecules that can escape as gases. The non-volatile components are primarily carbon-based and they are much lighter than the original material, causing further mass reduction.

It's trivial to say that the result as it is shown is not satisfying the demand as in we aim to have a compact non-porous substrate, but it is effective to see how the material shrinks during the process because of the burnt organic material and released gases especially during the pyrolisis.

In figure 2.4 it is clear how the lattice changes and passes from an amorphous state to a crystalline ceramic one. It can be appreciated that SiH groups clearly "disappear", being volatilized in the pyrolisis process, that also because of this makes the material lose weight and volume.

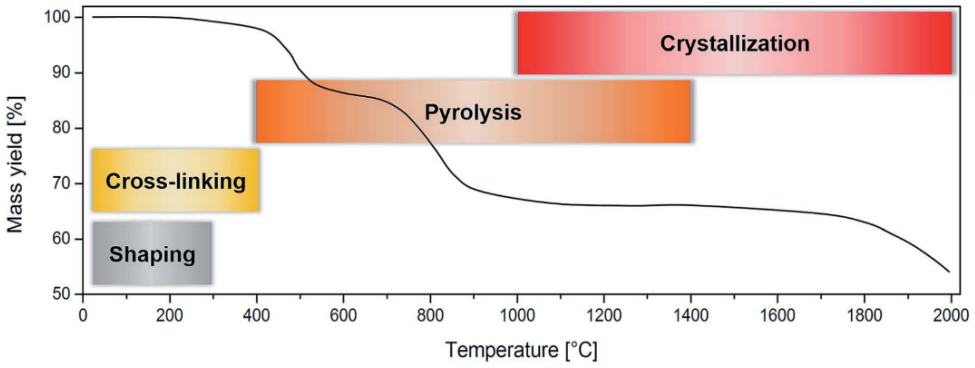

Figure 2.3: Mass reduction during the process [31]

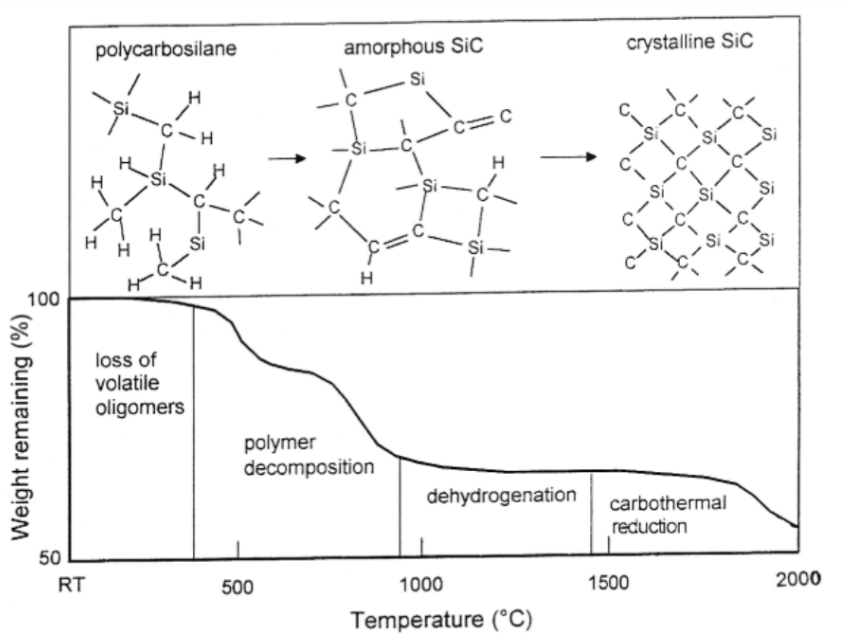

Figure 2.4: Structural transformation during the process for a PCS [36]

The carbothermal reaction does not concern the process here used, but it is defined as a type of chemical reaction where a carbon-containing compound, typically carbon in the form of coke, coal, or graphite, is used as a reducing agent to reduce metal oxides at high temperatures. This process leads to the extraction of metals from their oxides, releasing carbon dioxide or carbon monoxide as by-products.

2.1 Classification of preceramic polymers

As figuratively schemed in figure 2.1, preceramic polymers are classified based on their structure.

The simplest representation that describes every organosilicon polymers is in figure 2.5, where the variation of the X group results in different classes of Si-based polymers.

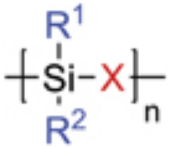

Figure 2.5: General oversimplified representation of the molecular structure of preceramic organosilicon compounds [33]

The chemical structures of these polymers are complex but can consist of linear, cyclic and branched units. Organosilicon polymers are mainly divided into polysilanes, polycarbosilanes, polysilazanes and polysiloxanes. [37]

An important value when talking about this kind of polymers is the ceramic yield (CY), defined as follows:

$$CY(\%) = \frac{R}{P}x100 \tag{2.1}$$

where R is the weight of ceramic residue and P is the weight of preceramic polymer.

2.1.1 Polysilanes

Poly(organosilanes) consist of a Si–Si backbone with organic groups attached to the silicon atoms. These materials have garnered significant attention due to their properties such as photoconductivity, luminescence, and high thermal stability, which arise from what is known as σ conjugation (single bonds formed by the head-on overlap of atomic orbitals).

Polysilanes have been utilized as functional materials in various applications, including semiconductors, photoresists, hole-transport materials, and precursors for silicon carbide-based ceramics. The first synthesis of poly(diphenylsilane) was achieved in 1921 by Kipping through a Wurtz-like coupling reaction of diphenyldichlorosilane with sodium in toluene. By the 1970s, several soluble homo- and copolymers had been documented. Despite the numerous advancements in the synthesis of polysilanes, the Wurtz-type reductive dehalogenation reaction remains the most widely used and general method for producing these polymers. In addition to the Wurtz coupling reaction, another method for polysilane production is the catalytically dehydrogenative oligomerization of hydrosilanes in the presence of transition metal complexes.[33]

2.1.2 Polycarbosilanes

Poly(organocarbosilanes) contain repeated units of Si–C bonds in the backbone. The molecular structure of polycarbosilanes is complex due to branched chains with crosslinks in the backbone.[37]

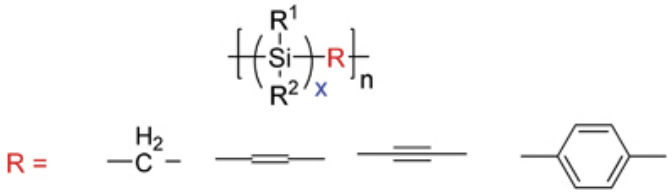

Figure 2.6: Polycarbosilanes simplified structure [33]

In paragraph 2.2 the material used in this set of experiments is elaborated, and it is part of this class of organosilicon polymers.

Polycarbosilanes have primarily been utilized for producing SiC-based powders, fibers, and their composites, which exhibit specific electromagnetic and optical properties. The solid polycarbosilanes developed by Yajima et al. in 1975 have been widely used as SiC ceramic precursors for more than 30 years. However, these materials have some drawbacks, including a low ceramic yield of 60% and the need for large quantities of solvent. To enhance the ceramic yield, olefinic side chain groups like vinyl, ethynyl, or allyl have been incorporated into the hyperbranched polycarbosilane backbone, which promotes sufficient cross-linking reactions at lower temperatures and results in ceramic yields of 70% upon pyrolysis. Further advancements led to the development and commercialization of allylhydridopolycarbosilane (AHPCS), marketed under the trade name SMP-10, which contains 5–10% allyl groups and produces high-performance SiC with an increased ceramic yield of 72% to 78%, along with shorter manufacturing cycle times.[37]

2.1.3 Polysilazanes

Poly(organosilazanes) contain Si–N bonds in their backbone with pendant groups which are typically hydrogen, alkyl and/or aryl groups. Commercialized polysilazanes with high thermal and chemical stability were developed.

The primary use of polysilazanes is as a preceramic polymer for the fabrication of SiCN and Si_3N_4 ceramics. They have superior properties such as excellent thermal stability, scratch resistance, corrosion resistance, high hardness etc., compared to polysiloxanes, thus they find applications as protective and heat resistant coatings in the electronics, automotive, aerospace industry, or as barriers for heat exchangers or on steel against oxidation.[37]

High ceramic yields are generally achieved from high-molecular-weight polymers. To increase the molecular weight of poly(organosilazanes) and improve the degree of cross-linking, various methods have been proposed. Significant efforts have been focused on modifying silazane oligomers into nonvolatile precursors. The various approach are listed by Colombo et al.[33]

2.1.4 Polysiloxanes

Poly(organosiloxanes) are important materials widely used for sealing applications. They are generally denoted as silicones and are usually inexpensive and a great variety of derivatives is commercially available. Many of them have excellent chemical, physical, and electrical properties.

The general synthesis method for polysiloxanes is the reaction of chlorosilane with water, according to the following reaction:

$$nSi(CH_3)_2Cl_2 + nH_2O \rightarrow [Si(CH_3)_2O]_n + 2nHCl \tag{2.2}$$

Chain polysiloxanes composed of difunctional units are produced, resulting in low molecular weight cyclic oligomers. These oligomers can then be converted into high molecular-weight viscous polymers through acid or base catalysis. It is common practice to use bifunctional silane precursors to synthesize linear and cyclic oligosiloxanes and polysiloxanes.

2.2 Process for polycarbosilane "Theton 3D"

The polymer chosen to realize the experiments for the purpose of the thesis work is a SiC precursor produced by the American company "Theton 3D" based in Nebraska (USA).

The precursor is sold charged with 60% of nanoparticles of SiC and appears as a dark grey, heavily viscous liquid. The slurry is an experimental resin produced directly from Tethon 3D and the exact composition is unknown for industrial purposes directed by the company.

The producers also gave precise instruction about the proper process to apply to the slurry, through an exchange of opinions with them, because, and that is due saying, the precursor is not originally thought as a joining material, but rather as a 3D printing resin.

The process, graphically represented in figure 2.7, is the following [38]:

1. 60 minutes of setting at 100°C in air furnace that constitutes the curing of the material, so when the polymer becomes hard
2. Linear heating with a ramp of 10°C/min until 800°C in tubular oven with Argon flux in inert environment
3. 60 minutes of isotherm

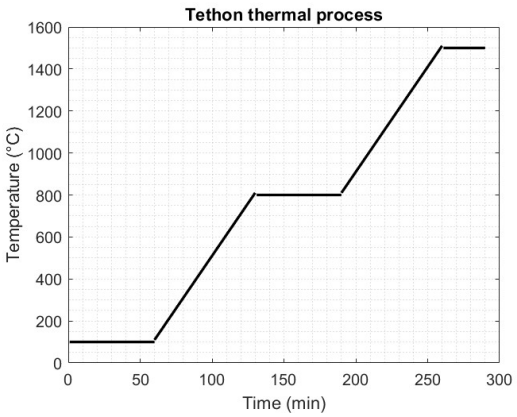

Figure 2.7: Thermal process for Tethon 3D

4. Linear heating with a ramp of 10°C/min
   until 1500°C in same conditions
5. 30 minutes of isotherm

The process is supported by and coherent with the patent by General Atomics (San Diego, California, USA), that is an invention with the purpose of providing high durability joints between ceramic articles, particularly βSiC and methods of making and using the same.

The process is divided in several steps[39]:

- preparing a slurry comprising a preceramic polymer and a plurality of inclusions;
- applying the slurry between the first and second articles;
- curing the slurry to form a green body;
- pyrolyzing the green body to form a solid ceramic containing the plurality of inclusions;
- converting the solid ceramic to a matrix comprising a crystallized ceramic polymorph and having the plurality of inclusions there
- reinforcing the joint by applying a sealant layer, which in one example is performed using chemical vapor infiltration to form a layer comprising a ceramic polymorph on the first and second articles and infiltrated into the matrix.

2.3 Process for solid polycarbosilane

It has been also tested a new type of polycarbosilane, supplied from WORLDEX Industry & Trading Co. (South Korea) with the peculiarity that it is solid, specifically with the aspect of a white powder. In this thesis, this material was not widely used, because it concerned only the last period of time.

The indicated process is the same as the Tethon slurry concerning the pyrolisis, but it is different (and slower) in the cross-linking treatment. Specifically, only the cross-linking process is reported in figure 2.8, and afterwards the process continues as in figure 2.7.

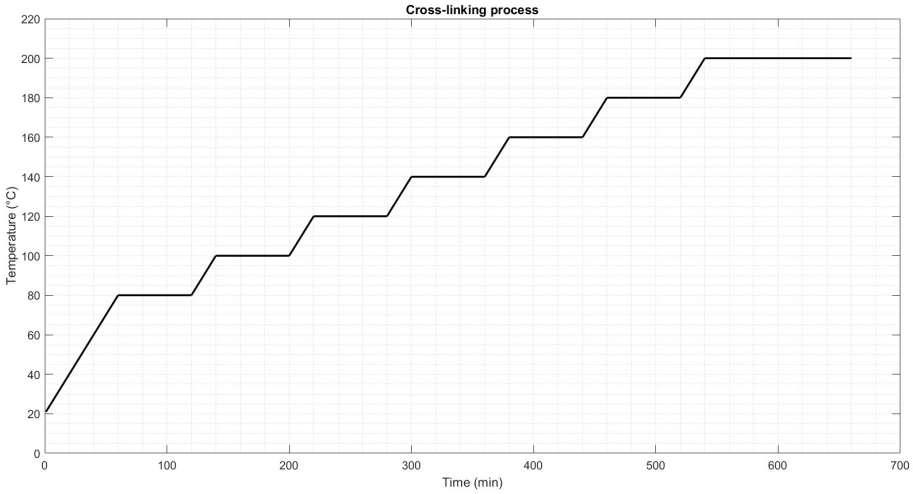

Figure 2.8: Thermal process for solid polycarbosilane

Considered that the material is a powder, it has to be diluted into a solvent to make a slurry in order to apply it similarly to the Tethon 3D liquid. The solvent to do so is hexane and the added quantity depends on the desired viscosity of the final product.

2.4 Fillers

In the context of materials joining, fillers refer to additional materials introduced between two components to facilitate the bonding process.

The use of fillers plays a pivotal role in these processes, influencing the mechanical properties, integrity, and functionality of the joint. Fillers bridge gaps, enhance strength, and enable dissimilar material joining, ensuring that parts remain securely bonded under varying conditions of stress, temperature, and environmental exposure.

Particularly, in this case study, fillers are of extreme importance to make the final piece a composite material, that in this situation requires a fiber reinforcement, and also they help to prevent an excessive volumetric shrinking and mass loss.

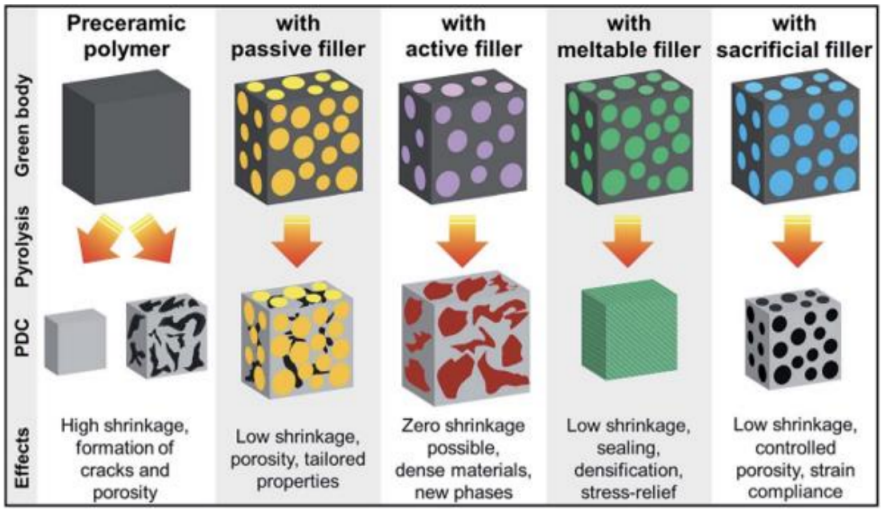

Figure 2.9: Differences in applications between different fillers type [31]

Fillers can be classified based on their interaction with the materials being joined into active fillers, passive fillers, and fusible fillers. Each type serves a distinct purpose in different joining technologies, as shown in figure 2.9. Understanding their properties and applications allows for optimized selection, improving joint reliability and performance. Fillers can also be classified based on their nature (ceramic, polymeric, metallic), morphology and size (powders, sheets, fibers at the nano/microscale).

2.4.1 Active fillers

Active fillers are materials that chemically react with the base materials during the joining process. These reactions occur at the interface of the filler and the substrate, forming new compounds that create a strong bond. The effectiveness of active fillers relies on their ability to wet the base materials and participate in chemical interactions, often producing inter-metallic or ceramic phases that enhance bond strength. The generic chemical reaction in inert atmosphere is reported in figure 2.10.

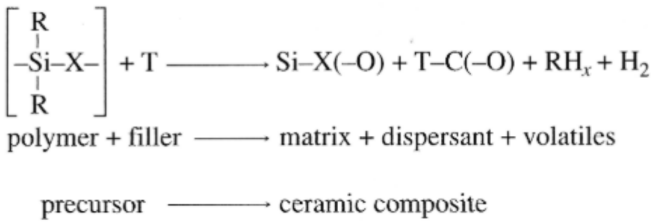

Figure 2.10: Reaction between a PDC and an active filler [40]

They are commonly used in processes such as brazing and soldering, where the filler must react with both materials being joined. For example, in brazing titanium or ceramics, active fillers like titanium-based alloys react with the surfaces to form strong chemical bonds. These active fillers enable the joining of materials that are otherwise difficult to bond, such as ceramics to metals.

Grain sizes typically range between 1 and 10 μm, with active fillers such as metallic particles (e.g., B, Ti, Cr, V, Mo) or intermetallic compounds (e.g., $MoSi_2$, $CrSi_2$) promoting the formation of metal carbides, nitrides, or silicides during pyrolysis through reduction reactions. These fillers provide significant benefits, including tailored electrical conductivity, enhanced magnetic properties, optimized thermal expansion coefficients (CTE), and improved mechanical strength and overall hardness.

However, despite these improvements, the presence of residual porosity can still have a notable impact on the mechanical performance of the material. The ability to balance property optimization while managing porosity is critical for designing advanced ceramics suited for high-performance applications in industries such as electronics, aerospace, and energy.

Active fillers can be used to introduce new phases into a polymer-ceramic system, modifying its functionality and performance. The formation of an additional stable or metastable tertiary phase, such as oxycarbides or carbosilicides, depends on the thermodynamic stability of the products obtained from the reaction between the polymer precursor and the active filler. Thermodynamic calculations identified optimal conditions for producing specific products, improving ceramic yield. Studies on a polysiloxane/chromium mixture showed that at pyrolysis temperatures below 600°C, methane is the main gas, leading to greater mass loss and higher porosity. Around 1200°C, hydrogen becomes the most stable gas phase, resulting in lower mass loss due to the smaller size of hydrogen compared to methane. The amount of residual carbon can be controlled by the quantity of added filler. At 1200°C, with 75% chromium, free carbon becomes thermodynamically unstable, and the stable phases in the final product are Cr-C and Cr-Si in varying proportions.[40]

Vijay et al. [41] experimented a $TiSi_2$ active filler applied in a BoSiVi matrix and obtained successfully ceramic nano-structures at 1500 °C and advanced MAX phase ceramics & UHTC phases in the temperature regime of 1800 °C to 2000 °C without the application of hot press technique.

Active fillers offer high bond strength and the ability to join dissimilar materials that would otherwise be incompatible. However, their application is often limited by the requirement for high temperatures and precise control over chemical reactions, which can complicate the process. Additionally, the formation of brittle intermetallic phases at the joint interface can be a concern in some cases.

2.4.2 Passive fillers

Passive fillers do not chemically interact with the base materials during the joining process. Instead, they act as mechanical support, filling gaps and distributing stress across the joint.

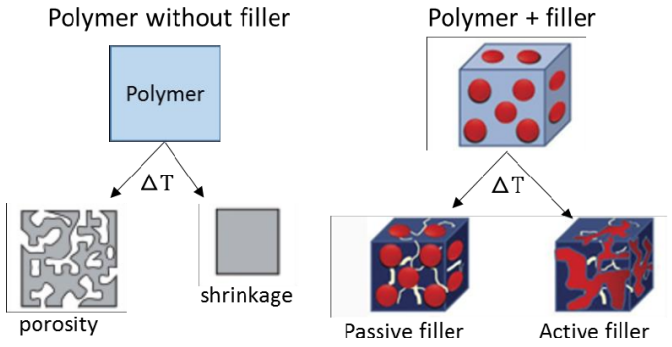

Figure 2.11: Comparison between active and passive filler [42]

The role of passive fillers is purely structural; they provide additional material that reinforces the joint but do not participate in the formation of new compounds or phases.

Passive fillers are often used in adhesive bonding and mechanical joining methods, where the primary function is to provide bulk to the joint or improve its mechanical properties without initiating chemical reactions.

These kinds of fillers are advantageous for their being inert at low and high temperatures without the need of a protected atmosphere. This feature makes the application of a passive filler simple, in no need of complex chemical reactions or precise temperature control.

In this thesis work the used fillers are going to be passive, specifically SiC fibers. That is because when dealing with polymeric precursors, as said, volumetric shrinking is an important factor to be reduced as much as possible, and a passive filler does not undergo shrinking, since it does not undergo pyrolisis. To sum up, a passive filler, due to its simplicity in application and being inert to most of the process conditions, maintains mass and properties between before and after the whole process.

As it is true that fibers are useful to reduce the total volume shrinkage, it is also true that the volumetric percentage has to be carefully chosen: adding the filler until 40-50% in volume averagely improves the cited properties, but bringing the percentage higher is detrimental and brings to a worsening of the joining because of the increase of porosity and also because a polymer low percentage is not sufficient to have a good wettability between the slurry and the substrate.

Generally, the physical properties of the passive filler must be compatible with the ones of the matrix, especially the thermal expansion coefficient, because considering all the changes the polymer undergo and the inert properties of the filler, a big discrepancy between the two material behaviors would cause cracks and eventually rupture of the joining.

2.4.3 Fusible fillers

Fusible fillers are materials that melt at relatively low temperatures and can be used to temporarily or permanently fill voids in a joint. Fusible fillers are often employed in processes where the filler material needs to flow into small gaps, fill complex geometries, or create a temporary support structure that can be later melted or removed.

Fusible fillers are widely used in welding, soldering, and casting processes, where their low melting point allows them to act as a bridge between two components. After cooling and solidification, the fusible filler forms part of the joint, contributing to its mechanical properties.

The most common type of material used for fusible fillers are glasses, that are supposed to melt (or soften) in the pyrolisis step. The softening helps also to reduce the thermomechanical stresses inside of the joining during the process and solidifying when cooled down gives hardness and resistance to abrasion.

Fusible fillers offer the advantage of low-temperature application, which is critical for joining sensitive materials, such as electronic components or thin metals. Their ability to flow into complex geometries and later become part of the joint is a significant benefit. However, their mechanical properties are typically lower than those of permanent fillers, and their use is limited to applications where high joint strength is not the primary concern. Another disadvantage of this technique is that the pyrolysis temperatures can lead to an excessive reduction in the viscosity of the molten glass or cause glass decomposition, while at lower temperatures the filler might exhibit only passive behavior, without showing any softening or melting.

Chapter 3

Experimental activity

The experimental part of the present thesis has been conducted in the laboratories of GLANCE (Glasses, Ceramics and Composites) group at DISAT (Dipartimento di Scienza e Tecnologia Applicata) of Politecnico di Torino and in the J-Tech@PoliTo (interdepartmental center focused on advanced joinings) under the surveillance of professor Monica Ferraris.

Inside of the research group, various activities are carried forward, including the use of glass-ceramic SAY, the use of different precursor such as silicon dioxide precursor through a PSZ instead of silicon carbide through a PCS, laser joining, and numerous other activities.

The activity was carried after all the due courses and security tests to work in them.

3.1 State of art of the activity

This thesis is the fourth one that faces experiments using Tethon as preceramic polymer inside of this research branch in Politecnico di Torino. Particularly, before this work, the topic was dealt by M. De Vivo [15], V. Pastorelli [43] and S. De Angelis [35].

They all had different experiences, since chronologically Tethon was more and more considered in time. With this it has to be said that none of them worked exclusively on this material, but they worked also on different techniques of joining: SAY glass-ceramics, laser, PHPS, silica precursor (Durazane 1800), YAG.

The results of the previous works never reached the goal of a proper cohesive and compact joining using preceramic polymers, but they were able to improve the technique and give a focus on the issues and the points of the process to refine.

Specifically, the joints present cracks and porosity at the end of every attempt. Nevertheless, there is still a deepening activity to do, because on a planar geometry the main activity so far focused more on coatings, and on the joining samples no mechanical tests were applied, so that the advanced study in the post-experimental phase of is still immature.

3.2 Cutting of SiC_f/SiC

The composite material for planar experiments is provided in large slabs that therefore have to be cut. [44] [15]

Figure 3.1: SiC slab

The cutting was made using the cutting machine Brillant 220 from QATM. [45] It is a machine that uses a rotating blade made for precision cut. The blade is continuously bathed by a double jet of distilled water to cool the blade and counterbalance the heat caused by the strong friction with the working piece.

(a) Brillant 220 before assembly (b) Removable components of the machine

Figure 3.2: Brillant 220

Considered the hardness of SiC/SiC, the used wheel was the one containing diamond powders, advancing relatively slow to safeguard the blade and the material from cracks, since both things

are very expensive components.

Specifically, the machine was used at the following settings: angular velocity of the blade of $3200rpm$, horizontal cut and forward speed of $0.030mm/s$. The result of the cutting is showed in figure 3.3.

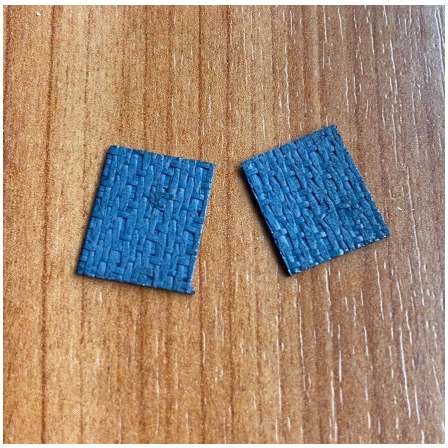

Figure 3.3: Cut pieces with measure 1.5cm x 1.5cm

3.3 Cleaning of SiC_f/SiC

The material after cutting must be properly cleaned before the experiment to avoid contaminations in the process.

3.3.1 Ultrasonic cleaning

The first cleaning process the component undergoes is an ultrasonic cleaning, in which the substrates are placed in ethanol inside of a becher and then they are put in a machine named Proclean 4.5S, produced by Ulsonix, that applies a cycle set manually of 10 minutes at 40°C.

The machine uses ultrasound with frequencies between $20kHz$ and $40kHz$ to agitate the liquid. The process works by converting sound energy into mechanical vibrations through a transducer. These vibrations are transmitted through the cleaning liquid, causing microscopic bubbles to form and collapse. This action effectively removes dirt and contaminants from the surfaces of objects placed in the cleaning tank. [46] The substrates must be carefully dried after the process to eliminate possible ethanol residues.

This way the substrates have an enhanced adherence on the surface and have less contaminants on the surfaces.

3.3.2 Plasma cleaning

In order to manufacture the final component, to itself or to other materials, is often necessary, and it is critical, to maximize the strength of the joints (similar or dissimilar) in order to meet reliability criteria.

The plasma cleaning works with the ionized gas (Argon) caused by the application of an electric field to the gas itself. The plasma interact with the surface and thanks to the high energy ions, the impurities leave it in different ways such as reaction with oxygen radicals and sputtering.

The presence of multiple constituents in CMCs introduces new opportunities for texturing via plasma etching. Indeed, the different set of properties, provided by each constituent, results in

a different response when the material undergoes a treatment enabling selective removal of the less resistant constituent and therefore providing texturing without masking. [47]

The machine was equipped with one nozzle and set at the conditions in figure 3.4.

	Generator	Nozzle
Main Voltage	220V	
Main Frequency	50Hz	
Output voltage	550 VA	425W
Ramp-up time	10ms	
Compressed air supply	5–6bar	

Figure 3.4: Technical specifications for the PlasmaTEC-X [48]

In figure 3.5 it is portrayed the nozzle of PlasmaTEC-X-OEM produced in Denmark by the company Tantec. As it is shown, the area hit by the jet is very limited, and that's why it was necessary to do multiple cycles in which the substrate was progressively slightly moved in order to clean the whole surface.

In the end, the treatment outcame this way: 5 cycles of 1 minute (60000 ms at the machine precision) each.

Figure 3.5: Plasma TEC-X-OEM

3.4 Preparation of the polymer and the filler

Theton 3D's material, from now on called "Theton", requires a proper treatment before being used for our purposes.

First of all, the material is conceived for 3D printing, and not to be used a a joining material in indirect joints. On the other hand, the company, with which it has been established a preventive contact to discuss the intentions and the feasibility of this study, assured that under the due circumstances the slurry can work as mean to the reaching of the goal of this thesis and research.

Theton is a very dense and viscous liquid already introduced and described in paragraph 2.2, aimed in this thesis to be smeared on a sample first planar, and then cylindrical in order to study its coating and joining properties on SiC/SiC as a representative of silicon carbide polymeric precursor.

Theton as a material itself has unknown composition, but it is to knowledge that it is already charged with 60% of ceramic SiC. That is not sufficient to overcome the big issue of the volumetric and weight reduction. In order to manually try to fix as fine as possible the problem, new fibers of silicon carbide were thought to be put in the slurry before the whole treatment as fillers.

The fibers were firstly tried to be synthesized in a previous thesis work through blocks of C fibers and Si wafers by gravitational force[35], but the result, although was not a failure, was not as pure as expected, because the fibers contained, in the end, a relevant percentage of pure carbon not reacted with silicon, that made the experiment not suitable for a nuclear grade application. The attempt, though, is not to be considered useless, because anyway a joining with mixed fibers of C and SiC in a SiC matrix can have various applications in other fields of industrial engineering, and C/SiC is a valid material to be considered after all in cases such as brake and clutch systems.[49]

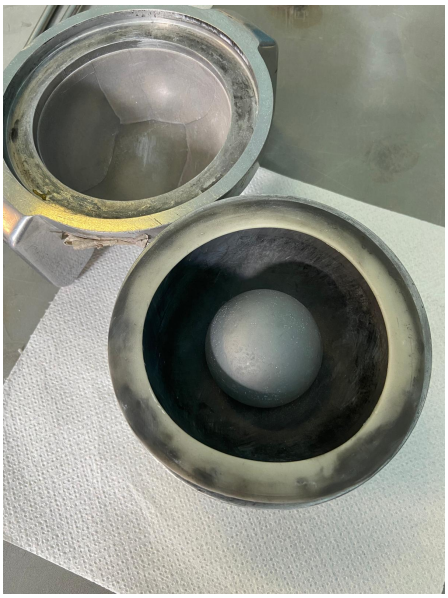

Figure 3.6: Grinder

The first experiments of this very thesis were done with fibers obtained by the grinding of SiC slabs: the result was not perfect, because the grinding gave out mostly powder more than fibers, but it was anyhow a good test considering that the result, whatever it is, would be 100% SiC.

The grinding was accomplished with the grinder machine in figure 3.6, in which a heavy ball bounces inside the crucible through an electric structure. The process was held for 20 minutes.

A powder filler is not ideal to our aim because a particle reinforcement is generally weaker than a fiber one: a particle reinforcement relies on making the path of the crack longer, while a fiber reinforcement works on the dissipation of the crack energy and the extinction of it, as shown in paragraph 1.3.

The choice of using the grinder can be imperfect in terms of result but it is surely cheap and it can be applied to scrap components. This added to the fact that it probably would not end up in being categorized as *nuclear grade*, but for other applications that allow a particles reinforcement the technique can be taken into account.

Afterwards, the work continued with the use of commercial fibers HI-NICALON type-S supplied

by CEA (Commissariat à l'énergie atomique et aux énergies alternatives) and produced by Nippon Carbon Co. The fibers arrived in the form of long fibers (stocks of 550m of fibers each), so they were cut in the laboratory with length comparable to the joining area's characteristic length. The used fibers, in the end, were the ones in figure 3.7

The adding of fibers can be done according to different criteria, but even though a rigorous mathematical approach would be the best option, the realization of that is difficult due to data scarcity about the used material. As a matter of fact, there is no precise information on the volumetric loss percentage post-pyrolisis, except for the indication that the polymer could reduce in volume up to 32%, but the different application used in this document results in various data. A TGA (Thermogravimetric Analysis) could be a way to solve the issue, but previous attempts failed due to the change of phase (from liquid to solid) giving only partially valid results.[15]

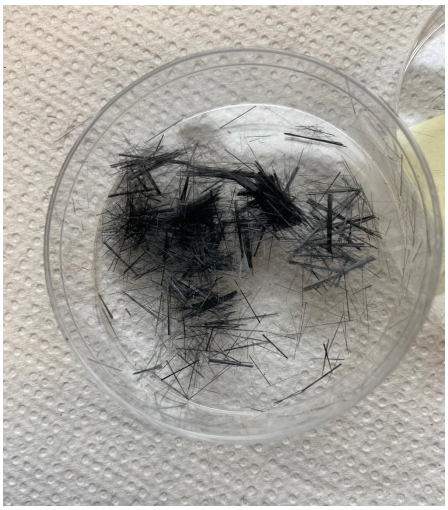

Figure 3.7: Hi-Nicalon type S fibers (Nippon Carbon Co)

In the end, an experimental approach was applied in the experiment, so the percentage of fibers charged to Theton was determined by trials. The measurements were done with a scale with an accuracy of 10^{-5} grams with a scale Radwag®.

Fibers (or powder) and Tethon must be well mixed to guarantee an equable distribution of reinforcement. In case of bad mixing, the final result would be unequal and would have zones in which the SiC is compact and nearer to the goal, but on the other hand zones with the same aspect as figure 2.2, naturally free of fibers, and so with heavy presence of creeps and porosity.

At this point, the surface is ready after the processes in paragraphs 3.3 and 3.2, and the slurry is ready. The next step is to apply carefully the viscous mixture over the substrates (in case of only coating there is only one substrate involved).

The step is achieved with the use of a spatula. A special care is needed in applying the mixture layer homogeneously, since the shrinking issue already gives inhomogeneity in itself.

When the situation is approximately like in figure 3.8a, the sample is ready to be put in the oven in case of a coating experiment. In case of a planar joining test, the process must be applied to the two substrates and then they must be jointed as figure 3.8b shows.

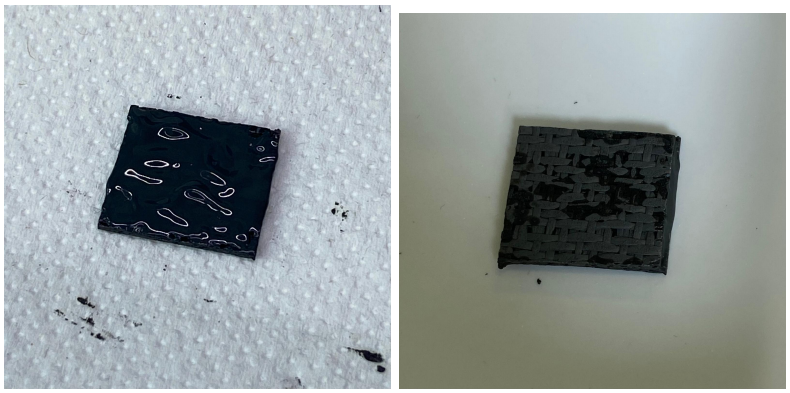

(a) Coating (b) Joining

Figure 3.8: Systems ready for the thermal process

3.5 Thermal process

The thermal process to convert the polymer is explained in paragraph 2.2 and it is suggested by the company Tethon 3D. In figure 2.7 the thermal profile the sample undergoes is ideal and precisely between the curing step and the pyrolisis the system is cooled down gradually with standard environment.

3.5.1 Curing

The curing step is performed in a Binder oven with air flux, pre-heated at 100°C to follow the indications. During the process, during some of the tests, in the joining cases, a weight has been applied over the joint in order to guarantee adhesion between the substrates and the slurry.

Curing had a timing of one hour as indicated except for some attempts in which it was prolonged to 1.5 hours to try to have a better cross-linking and so a more solid result. This attempt of improving the process in the first phases was undertaken after seeing that in the curing step the slurry did not cross-link, as it was still having a fluid aspect and behavior. The idea came after assuming that the process introduced in chapter 2.2, indicated exactly for the Tethon 3D polymer, was given for a coating approach, but in joinings the thermal transmission is not homogeneous because the temperature takes more time to reach the middle of the joint.

To avoid the formation of cracks the air oven for the first step is maintained closed for several hours after the curing to have a homogeneous cooling and not cause thermal shock.

3.5.2 Pyrolisis and crystallization

These steps are performed in Argon in inert environment to avoid oxidation and contamination during the process. The used machine is an oven produced by XERION, at the J-Tech@PoliTo laboratory, able to reach temperatures up to 1700°C with a heating rate of 10 K/min and a void of $5\text{x}10^{-6}$mbar. [50]

These steps as well are achieved with the help of a weight to keep the joint in place, but in this case the weight is of tungsten for its thermal properties. A gradual cooling at the oven pace is applied here as well, before the re-pressurization of the chamber to avoid cracks due to thermal shock.

3.6 Re-infiltration

As already explained, one of the main problems of the polymeric precursor technology is the porosity afterwards and generally the gap between the volume occupied and the theoretical volume (m/ρ) due to the shrinkage during the process, mainly in the sintering part.

Often the simple adding of the fibers is not sufficient to fill all the voids in the joining material, so it is necessary to execute a re-infiltration. The aim is to apply a second time (and more if necessary) the polymer on the joining and repeat the whole thermal process in order to attempt a reduction of the voids and an increase of the total density.

The operation is quite simple if it is executed on a coating sample, because it is sufficient to apply the polymer with a spatula once again and repeat the process in the two ovens. If the sample is a broken joined sample, the process is simple as well because one of the faces needs to be coated again with the slurry without the need of surface cleaning and then the joining is to be done again. This has been done in the TT4 to TT5 test in this thesis work (see chapter 4).

In the situation in which the joint did not break or in the tube-cap experiments, the operation is much more problematic, because there are no joining areas available for the re-application of the slurry with a spatula. The proposed operation is to dip the samples in the polymer with a suitable viscosity and re-infiltrate by capillarity through the pores.

3.7 Characterization

The activity consists of the observation of the microscopical structure and the elements composition. The whole process is done through a preparation of the surface to be analyzed and the use of electron microscopy (SEM and FESEM).

This part is pivotal to understand if the joining was a success, considering the conditions of cohesion and adhesion required.

Further analyses include the CT scan, which uses X-rays to examine the internal adhesion of the joint, and finally, the mechanical tests, which in this work are destructive and are used to produce a stress-strain graph to characterize the mechanical behavior of the material. These final tests were performed exclusively on the tube-cap samples, as they are the primary experimental outputs of this research.

3.7.1 Incorporation in resin

Due to the high cost of the materials, the samples are small, just enough to have a complete and relevant knowledge of the obtained result. The substrates in the planar trials are squared with area 1.5x1.5 cm^2, that is a dimension too small to be treated without a physical support. So, the joining had been incorporated in a plastic resin with a circular die with a diameter of 3 cm as in figure 3.9.

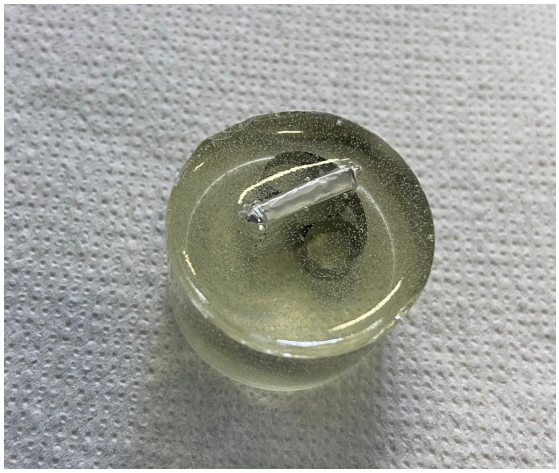

Figure 3.9: Sample incorporated in resin

To avoid permeation of the resin in the joining area, since it is liquid before the cross-linking, the sample was wrapped in an Aluminum foil, (figure 3.9).

The 8-shaped pattern in the figure is a clip used to stabilize the sample in vertical orientation during the long process of cross-linking of the resin.

The resin was obtained through a cross-linking process under the hood for about 72 hours and then cut in the Brillant 220 cutting machine. This step is important to get a view of the cross section of the joining: the edges of the sample are affected by the imperfection of the spatula application resulting in dishomogeneity and porous surface. On the other hand, with a transverse cut, the surface of the cross sections gives an useful view for analysis as the joining is achieved in the central parts.

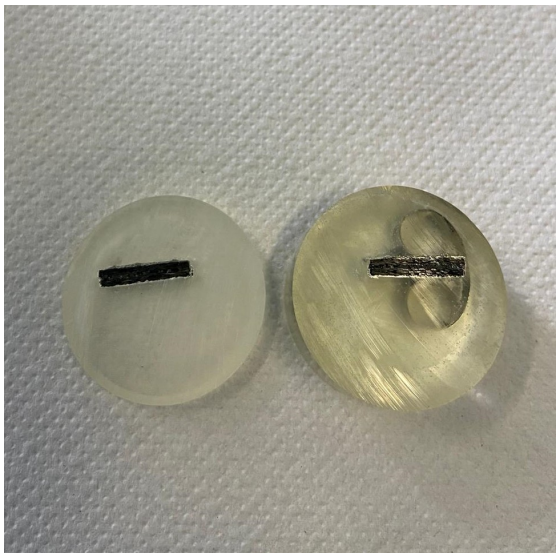

Figure 3.10: Samples wrapped in Al and embedded in resin

3.7.2 Polishing

When it comes to microscopical analysis, polishing is a very important step. Effectively, the system as just cut is far from perfectly smooth on the surface, even though the cutting was made with diagonal cut at 0.005 mm/s, that is, a relatively very small moving speed of the blade.

So, this step is important because using high precision microscopy, particularly using electrons, even an apparently small roughness make the scanning useless, as the focus will not be appropriate on the whole analyzed surface.

Polishing is achieved to a polishing machine, composed by a rotating polish paper and water for cooling. The polishing was a process composed by several steps, as to arrive to a fine result it would be very difficult taking directly the polish paper of the wanted precision. So, different polishing paper were used, from the coarsest to the finest. The criterion used to define how coarse is the polish step is the grit number, defined in Europe through the FEPA scale. In table 3.1 the different FEPA values of the papers used in our tests and the corresponding values of the average diameter of the roughness clusters are listed.

Every time the paper was changed, the sample was rotated by 90° in order to avoid preferential direction of the scratches caused by the polishing and to get rid of them.

FEPA	
Grit number	**μm**
P120	127
P400	35
P800	21.8
P1000	18.3
P1200	15.3
P2500	8.4
P4000	5

Table 3.1: Graded papers levels

3.7.3 Scanning Electron Microscopy (SEM)

Theoretical background

A Scanning Electron Microscope (SEM) is an advanced imaging tool used to analyze the surface topography and composition of materials at the micro- and nano-scale. It operates by scanning the surface of a sample with a focused beam of electrons, rather than light (as in optical microscopes). SEM is widely used in materials science, biology, and engineering due to its high-resolution imaging capabilities.

The SEM used for this work in GLANCE laboratories has a filament gun to produce electrons (they can also be produced by a high electric field) made of tungsten. The electrons are accelerated through a potential difference and through electrostatic lens they are focused on the target on a very fine point.

When the electron beam interacts with the sample, a "pear-shaped" volume in depth is taken into account. The volume is divided into 3 sections, each one devote to a different type of detection, as it is visually explained in figure 3.11. The X-rays are not of interest in this case study, but it is worth an in-depth analysis of the first two sections of the interaction volume. Every section has a dedicated detector placed in precise positions inside of the chamber.

Secondary electrons (SE) are generated when the primary electron beam interacts with the atoms in the sample, specifically when it displaces loosely bound electrons in the outer shells of the atoms (valence electrons). The electrons from the beam have high energy, and some of them excite the surface atoms through inelastic scattering and make them eject electrons with low energy, that are what we call the secondary electrons.

Because these electrons come from near the surface, they provide high-resolution images that are rich in surface details. The detector is as well near to the surface to collect the low energy electrons. SE images provide information about the morphology and the texture with great detail.

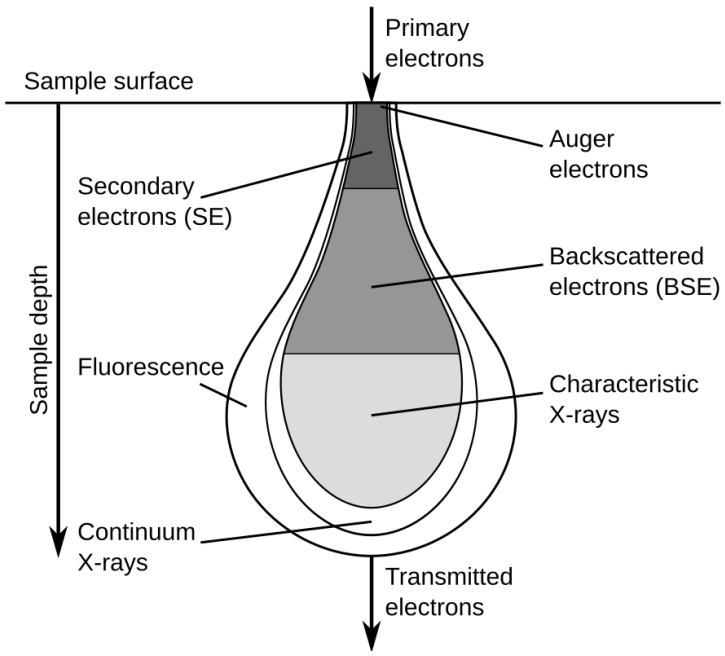

Figure 3.11: Interaction volume in SEM[51]

Going further in the interaction volume, the back-scattered electrons (BSE) are the result of elastic scattering interactions, where the primary beam electrons collide with the nuclei of atoms in the sample. The energy of these electrons remains relatively high (greater than 50 MeV).

This means that the electrons collected by the detector are exactly the same of the primary electron beam, simply back scattered from the elastic collision.

Because BSEs come from deeper within the sample (relative to secondary electrons), they provide information about both surface and subsurface features. About this, heavier elements allow a better scattering, while the one from light elements is weaker, so regions with heavy elements appear brighter, while lighter elements appear darker. This detail allows the detector to determine, even if not perfectly, the chemical composition of the sample (except for H, He and Li because too light [52]), once tabulated the intensities of the BSEs and linked to the relative chemical element. This feature is very useful in this very thesis work because it is important to determine if the precursor transforms entirely into SiC.

Practical use of SEM

Because SEM uses electrons as mean of analysis, it is fundamental to have a completely electrical conductive material. Since the sample was incorporated in resin, which is plastic and so not conductive, the system was metallized. Metallization is a procedure that deposit, through sputtering, a conductive material over all the surface of the sample, using a specific machine. The chosen process sputters a layer of 3 nm of thickness of chromium, in vacuum chamber using plasma.

Once the system is conductive, it can be placed in the SEM chamber, as shown in figure 3.12, at the center of the available target surface and fixed with screws.

Figure 3.12: Placing of the sample inside of SEM

It has been said that the electrons are accelerated with the application of a potential difference. The higher is the voltage applied, the deeper is the interaction of the electron beam and the more details is possible to extrapolate in the image. Particularly the SEM used in the laboratory offers 3 possible high voltage settings: 5 kV, 10 kV and 15 kV.

Voltage	5 kV	10 kV	15 kV
Penetration Depth	Shallow, near-surface imaging	Moderate penetration	Deeper penetration into the sample
Interaction Volume	Small (surface-sensitive)	Medium	Larger (bulk-sensitive)
Resolution	High for surface features	Balanced between surface and depth	Lower for surface but better for bulk
Secondary Electrons	Dominant (good surface detail)	Moderate contribution	Reduced contribution
Back-scattered Electrons	Minor contribution	Moderate contribution	Dominant (good for compositional info)
Compositional Contrast	Weak	Medium	Strong (especially for heavy elements)
Sample Charging	Minimal (best for non-conductive)	Moderate	Significant risk for non-conductive
Sample Damage	Low	Moderate	Higher
Suitable for	Surface-sensitive imaging, biological, non-conductive samples	General purpose imaging with good balance	Compositional analysis, deeper imaging

Table 3.2: Comparison of SEM performance at 5 kV, 10 kV, and 15 kV

A scanning with 5 kV in this case is important to analyze the secondary electrons, so to have a high quality of the surface resolution, having the possibility of studying the texture.

A 10 kV voltage allows to have a balanced analysis, but the penetration depth of the electrons is not yet very accurate in the analysis of BSEs behavior, so the compositional information, despite being available, is not accurate.

A 15 kV voltage, on the other hand, gives a dominant contribution of BSEs, so the compositional information is accurate, with the said limits, and the interaction volume is bulk-sensitive, together with a deep penetration into the sample.

Table 3.2 shows a summary of the features at the three different voltages making a comparison. During the SEM analysis in this work all of the three were used for different purposes.

3.7.4 Computed Tomography scan (CT-scan)

A Computed Tomography (CT) scan, originally developed for medical imaging, has become an invaluable tool for the non-destructive testing and analysis of materials. The technique utilizes X-rays to create detailed cross-sectional images, which are then digitally reconstructed into a three-dimensional model of the object under study. This allows researchers to visualize the internal structure of materials without altering or damaging them, which is crucial in fields such as materials science, engineering, and archaeology.

CT-scan works by rotating the X-ray source around the material while detectors capture the transmitted radiation. The density and composition of the material affect how much X-ray is absorbed, resulting in varying levels of contrast in the images. These multiple 2D images are compiled by computer algorithms into a high-resolution 3D representation, enabling detailed examination of internal features such as voids, cracks, inclusions, and phase distributions within the material.

In materials science, CT-scan is applied to study the microstructure of composites, metals, ceramics, and polymers. For example, it allows to inspect fiber-reinforced composites, identifying any defects or misalignments in the fiber arrangement that could impact mechanical properties. In metals and alloys, CT scanning can detect porosities or inclusions that may weaken the

material. Understanding these internal flaws is essential for improving manufacturing processes and ensuring product reliability.

In this thesis CT-scan was used to study the porosity inside of tube-cap joinings before eventually break the joining with mechanical tests. If the CT-scan result presented pores or cracks, a reinfiltration is necessary to cover the voids.

The equipment was designed by Fraunhofer IKTS for J-Tech@PoliTo. Its main features include a maximum applicable current of 1000 µA, a maximum voltage of 300 kV, and a 4-axis manipulation system that allows complete movement of the sample along the xyz Cartesian system.

3.7.5 Mechanical tests

The mechanical tests on the samples were done only on tube-cap joinings in collaboration with the J-Tech@PoliTO team.

The machine used in their laboratories to compute the stress-strain relationship was supplied by Zwick Roell and worked by using a linearly increasing rate of force applied to the sample through a couple of presses.

In figure 3.13, it is shown how the machine works: it is a vertical high precision test that pushes down the cap from the inside after gluing the sample to the structure in order to have an adhesion strength supposedly greater than the joint strength.

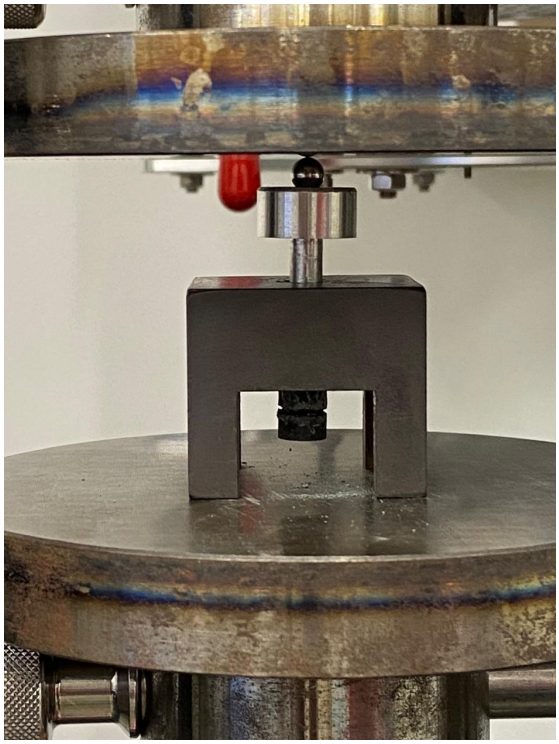

Figure 3.13: Mechanical test machine

The tests are defined as destructive because the tube and the cap eventually separate when the joining breaks. In addition to output the maximum force the sample can withstand, the stress-strain graph gives information also about the plastic behavior and the maximum $\epsilon\%$ before the rupture.

The tests also allows to have a uniform rupture surface to be analyzed, for example to evaluate,

in addition to the cohesion of the polymer, the adhesion of it to the sample surface, that can be eventually further analyzed with SEM.

After the test is done, the sample is still glued to the structure, as in figure 3.14, so the system needs to be put in the oven to melt the glue and take out the sample.

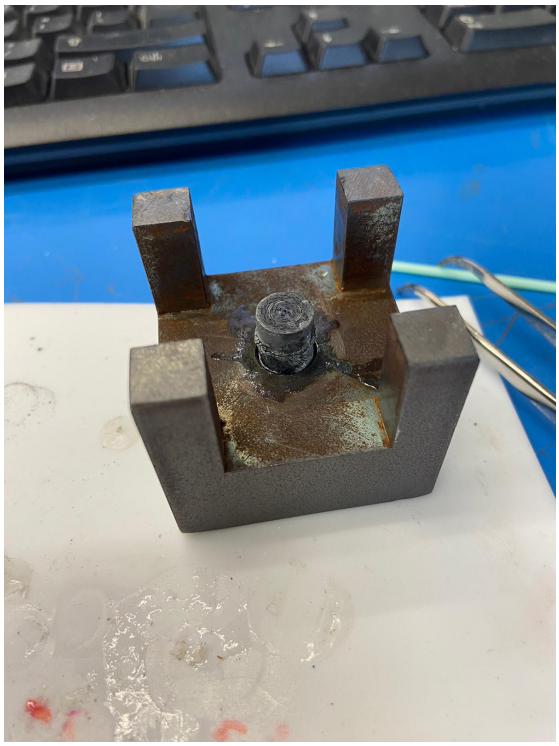

Figure 3.14: Joined sample in the fixture for mechanical test

Chapter 4

Results

The experimental activity is aimed to analyze the behavior of the polymeric precursor after the pyrolisis and within the process, and to find the right methods and procedures to get to a SiC_f/SiC joining. Particularly, the final product is supposed to be the joining between a cylinder and its cap (supplied by CEA through the IL TROVATORE European project), of which attempts are illustrated in section 4.3.

Before experimenting that particular geometry, a preliminary study using planar geometry is executed, on substrates as the ones in figure 3.3. The substrates, cut from the slabs, are used in two ways: for coating, to visually experiment and analyze the behavior of the polymeric precursor during and after the thermal process, and for joining, using two substrates.

One key factor affecting all three types of experiments is the ratio between the polymer matrix and the fiber reinforcement. The experimental approach shifted significantly when the SiC grinding filler was replaced by Hi-Nicalon Type S fibers. It was discovered that the Hi-Nicalon fibers required a much lower mass fraction to achieve the same volume within the composite. This is because these fibers are less dense than the ground SiC filler, meaning a smaller mass of Hi-Nicalon fibers could occupy an equivalent volume in the composite matrix.

The different single experiments will be referred, from now on, as TTn, were n is the chronological number of experiment during the experimental activity.

Name	**Type**	**% fibers (weight)**
TT0	Substrates	16.3
TT1	Coating	0
TT2	Coating	0
TT3	Substrates	24.6
TT4	Substrates	8.2
TT5	Substrates (re-infiltration)	1.3
TT6	Substrates	1.3
TT7	Substrates	1.3
TT8	Tube-cap	1.3
TT9	Tube-cap	4.1
TT10	Coating	4.1
TT11	Tube-cap (re-infiltration)	23.5
TT12	Coating (re-infiltration)	23.5
TT13	Tube-cap	2.3
TT14	Coating (re-infiltration)	2.3
TT15	Substrates	2.3

Table 4.1: Experimental activity

To provide a comprehensive overview of the experimental activity, table 4.1 lists all conducted experiments, specifying the type of experiment (coating, substrate, or tube-cap) and the weight percentage of fibers added to the precursor material.

It is important to note that, starting from sample TT4, the fiber weight percentage changed significantly due to variations in fiber density, as previously discussed. Additionally, samples TT5 through TT8 used the same slurry mixture, maintaining a consistent fiber percentage across these experiments. TT0, included in the table, represents a preliminary training test on substrates.

4.1 Coating

Coating samples can give important information about the behavior of the polymer. As a matter of fact, a coating test is the only way to easily see process transformation such as the volumetric reduction.

TT1 and TT2 were two coating experiments composed of all the steps of the thermal process, so until the complete pyrolysis. The experiment was done with the pure Tethon 3D fluid without further fillers (it has to be reminded that the slurry already contains nano-particles of SiC as explained in 2.2), because the point of doing these tests was to observe the behavior of the product on a free surface before and after the pyrolysis, and especially to acknowledge the volumetric shrinkage in a quantitative way and have an idea of the filler amount that would be needed.

The slurry was applied and the result is shown in figure 4.1. It was applied all over surfaces with a good homogeneity after the two surface cleaning treatments (ultrasonic and plasma).

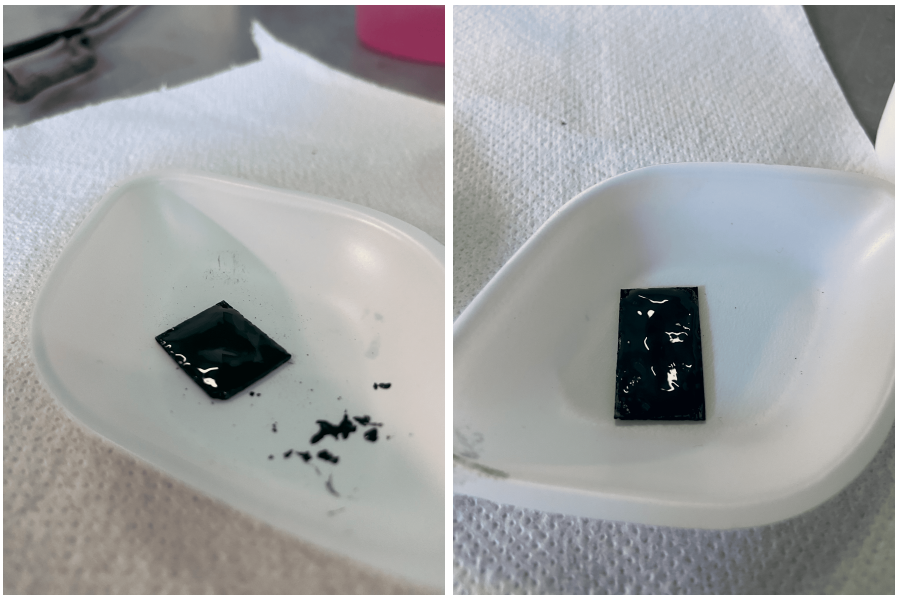

(a) TT1 (b) TT2

Figure 4.1: Slurry application

After the first step, 1 hour at 100°C, it has been noticed that the joining material did not solidify at all, but rather it looked the same in color and consistency. The same behavior was observed in the previous works about this particular material [35], so it has been assumed that it is typical of the used polymer. The reason could be that the cross-linking is supposed to happen

at higher temperatures. Further researches could deepen the topic, for example examining the post-curing samples at SEM or with similar techniques.

After the treatment in the XERION oven with Argon flux (after the curing step, in figure 2.7), pyrolysis and sintering process were completed, and the organic components were completely burnt, leaving as a residual only SiC obtained by the polymeric precursor, result in figure 4.2. The most noticeable features and defects of the coating are the cracks and the low tendency to be cohesive and adhesive to the surface, that is cut SiC/SiC.

Figure 4.2: Coated SiC/SiC with pure Tethon 3D slurry (TT1 and TT2)

To give an idea of the adhesion problems with this coatings, the obtained scales of SiC would just detach by gently scrape the surface, resulting in an almost clean surface, as if it was not treated.

After these results it was obvious the necessity of adding fibers to the fluid. As we will see, the filler will drastically improve the cohesion of the joint.

The most functional way to see the improvement that the fibers bring was to make another test with filler when the new fibers Hi-Nicalon type-S were available, and that was the trial TT10. The experiment TT10 was done with a filler mass percentage of 4.1% with purely Hi-Nicalon type-S fibers.

The result, in figure 4.3, presented an aspect still with a heavy presence of cracks in the surface and inhomogeneities, but anyway with a noticeable improvement in the cohesion and above all in the adhesion to the substrate. As a matter of fact, while in the tests without added filler the SiC would simply scrape off from the surface, in TT10 all the scales remain attached to it even soliciting them with a spatula. When they eventually detach from the surface, they are bonded by the fibers presence, so they move in clusters, showing that when the adhesion fails, a cohesive behaviour is achieved through the long fibers.

Figure 4.3: TT10

The sample TT10 showed good results and improvements, but it is clearly not a satisfying coating in terms of homogeneity, and that is why it has been decided to re-infiltrate it as in TT12.

The re-infiltration TT12 was done with a mixed filler in order to test the coexistence of powder and fibers reinforcement, of which the weight percentages are reported in table 4.2. As powder it has been used the same ground mixture of SiC/SiC obtained with the laboratory's grinder. Once again, the powder mass percentage is much higher than the fibers one because the powder comes from a ground massive sample.

Powder%	**Fibers%**	**Total%**
17.6	5.9	23.5

Table 4.2: TT12 re-infiltration filler composition

The result of the experiment, in figure 4.4, was good and promising: the re-infiltration gave as a result a much more compact surface, together with an enhancement in the cohesion and adhesion to the surface. The presence of fibers is evident, even though the upper limit was not reached, as in they were sometimes localized in clusters leaving some areas lacking of filler.

These considerations were achieved through a preliminary analysis carried out with an optical microscope, of which some snapshots are showed in figure 4.5.

The improvement was evident (the comparison is to be done with TT10 in figure 4.3), because despite the presence of cracks did not disappear, they reduced in dimension and depth, and there was a high chance that the surface had a complete coating without holes all the way to the bare surface.

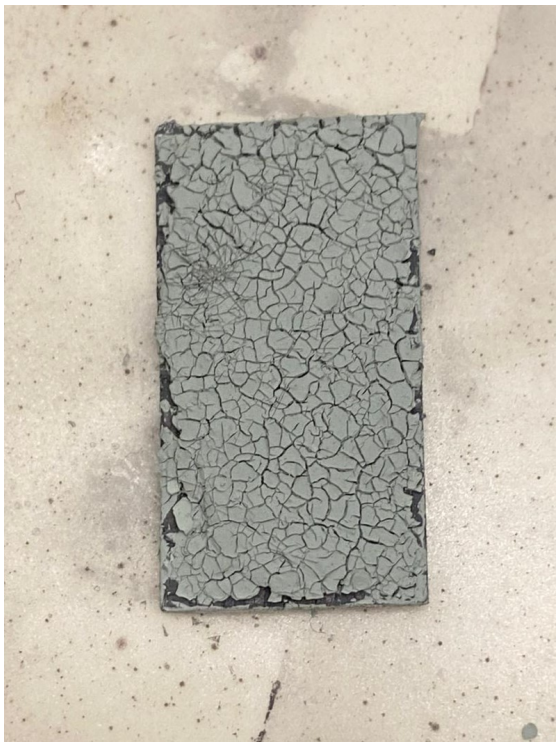

Figure 4.4: TT12

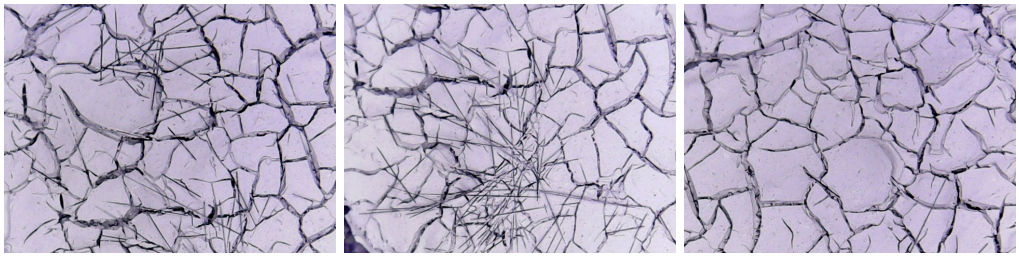

(a) (b) (c)

Figure 4.5: Microscopy of TT12

The sample TT12, even if considered a satisfactory result, was re-infiltrated (TT14) a second time to get an even more cohesive coating. In this experiment, together with the tube-cap joint TT13, a new curing process has been tested, in order to attempt to overcome the problem that arose regarding the lack of cross-linking after the curing step introduced before: after the due consultation, it was decided to increase the temperature and the stove time in the whole pre-pyrolisis process.

So, the specifics of the curing process were a ramp from room temperature to 200°C in about 20 minutes, and a hold at regime T for a total step time of 2 hours. The sample was then maintained in the stove to have a gradual cooling.

The result of the curing was satisfactory: the slurry solidified, as figure 4.6a well shows, that means that this new adopted process works and it is suggested to use. The slurry mixture for this attempt contained 2.3% of Hi-Nicalon type-S fibers ∼1 cm long.

Figure 4.6b shows the results of the experiment after pyrolysis. Given that this is the third re-infiltration since sample TT10, the outcome provides insight into how repeated infiltrations

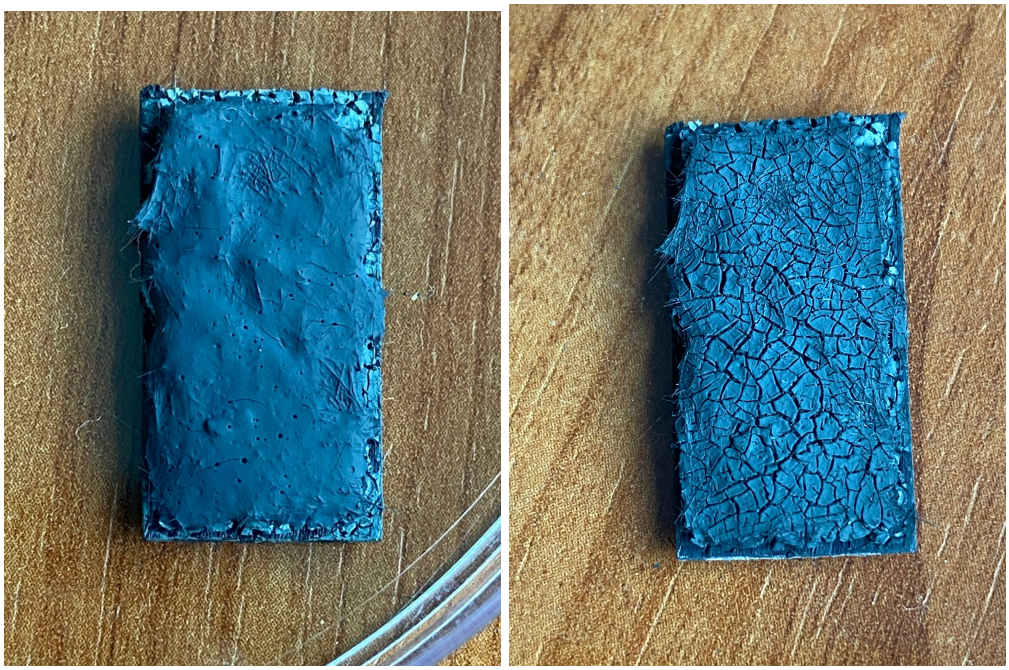

(a) After cross-linking (b) After pyrolysis

Figure 4.6: TT14

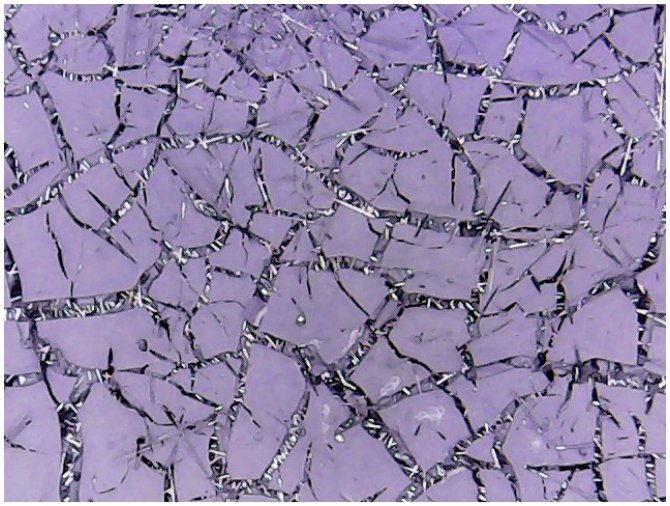

Figure 4.7: Microscopy of TT14

improve the cohesion of the coating. Future SEM characterization could confirm whether a uniform coating has formed over the entire surface, indicating that all voids have been adequately filled.

Figure 4.7 presents a microscopy image of sample TT14, illustrating how the fibers contribute to material cohesion by filling voids created by volumetric shrinkage. The cracks appear less pronounced, indicating effective fiber reinforcement within the matrix.

4.2 Joining of SiC/SiC slabs

The joining experiments on SiC/SiC slabs were done to test the different parameters of the process, such as the polymer-fibers ratio, the curing time and the thickness of the joint, because slabs are cheaper and easier to clean to try again in case of failure. All these trials were done with the aim of finding the optimal conditions for the joining slurry mixture.

Of the six attempts, two joints, TT0 and TT4, broke right away, meaning that they would break with a manual shear stress applied. The other four attempts were worth of morphology studies, so they were analyzed at SEM. All of the tests were done on 1.5x1.5cm^2 substrates of SiC/SiC.

The very first attempt of this whole work was the test named TT0, that as said was just a training joint, made with a mixture with 16.3% of fibers and the rest of Tethon 3D. The joining after the process broke with a simple hand-strength shear stress. The result was anyway helpful in order to understand the procedures and the errors. The two surfaces after the failure showed a low adhesion to the polymer and inhomogeneity in the distribution of it, and after a microscopical evaluation it has been understood that a coating was not achieved as well because part of the original surface is exposed.

Figure 4.8: Surface detail of TT0

The described peculiarities of TT0 test are clearly noticeable in figure 4.8: the fracture surface is rough and not well distributed, together with the fact that the polymer layer is too thin and makes the substrate visible. In this sample the filler consisted of the powder obtained by grinding SiC, so the low presence of long fibers made also the cohesion problematic.

To sum up, TT0 had many problems, that in the subsequent tests were attempted to be solved by increasing the quantity of the mixture in the joining area, increase the volumetric presence of the SiC fibers, change the fibers, apply the slurry more homogeneously and focus on an accurate cleaning of the surface, especially during the plasma etching process (section 3.3.2, where because of the reduced dimension of the nozzle it was difficult to have an efficient cleaning on the whole surface.

The next planar joining test was TT3, with an added fibers fraction of 24.6%; the percentage is much higher compared to TT0 for the reasons explained before, in the attempt to have a better adhesion and cohesion. After pyrolysis the sample was clearly more resistant than the previous one, because it did not break and it looked solidly joined.

Given the promising aspect of the sample, it has been decided to analyze the sample with the SEM. So, it was incorporated in resin, and after the cross-linking, it was cut with Brillant 220 cutting machine as in figure 3.10 and gradually polished until a P4000 grit number (see table 3.1). Successively it was metallized with chromium and finally analyzed at the electron microscope.

The focus was on verifying that the polymer transformed in SiC and the to see the adhesion and the porosity of the joining. About the first point, the result was satisfactory: increasing the SEM voltage to 15 kV, it has been possible to perform an EDS compositional analysis, that gave as a result the graph in figure 4.9, with the composition in table 4.3 detected in point 005, in figure 4.10a.

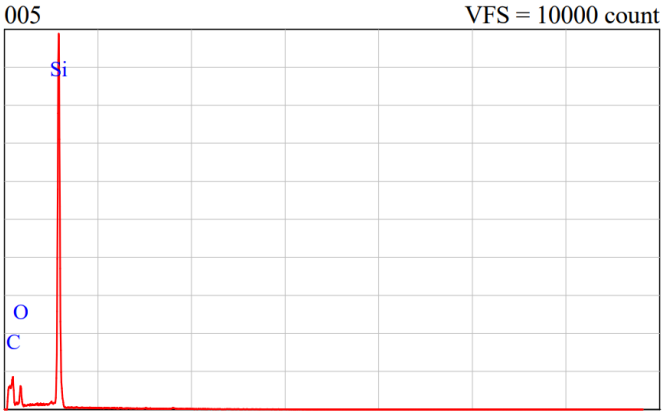

Figure 4.9: EDS compositional analysis of TT3

Element	keV	Mass %	Atom %
C	0.277	26.45	43.71
O	0.525	8.11	10.06
Si	1.739	65.44	46.24

Table 4.3: Compositional analysis of TT3

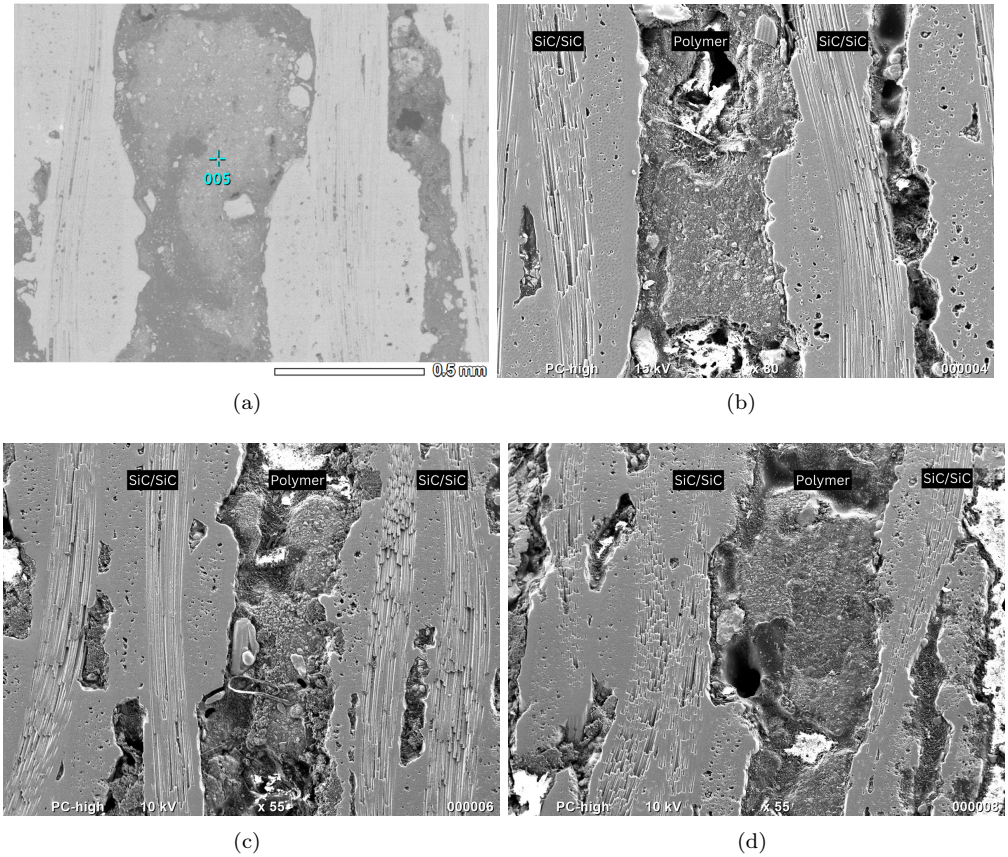

(a) (b)

(c) (d)

Figure 4.10: SEM images of TT3

The aspect is compact but the presence of actual fibers is rare: there is a clear example of it in figure 4.10c, but everywhere else it is a powder reinforced material. Nevertheless, it is appreciable the low presence of pores and an apparent good adhesion between the polymer and the substrates.

The first sample with the Hi-Nicalon type S fibers, TT4 was a failure, and the reason is to be attributed to a too high amount of fibers. Even if the weight percentage is drastically lower, as said, the relative volumetric percentage was higher than the TT3 sample, and the fact that the fibers were cut with an approximate length of 1 cm, required a more careful mixing of the slurry. These were the reasons why the sample broke after the pyrolysis.

TT4, in figure 4.11, gave as a result lots of fibers in the rupture area not bonded to the polymer nor the substrate, and under that layer, porous SiC obtained from the polymer.

More specifically, in figure 4.12, it is showed a view of the surface using an optical microscope where is clear that the fibers did not have a bonding function and improve adhesion and cohesion, but rather they made it worse because they did not allow the slurry to properly wet the surface.

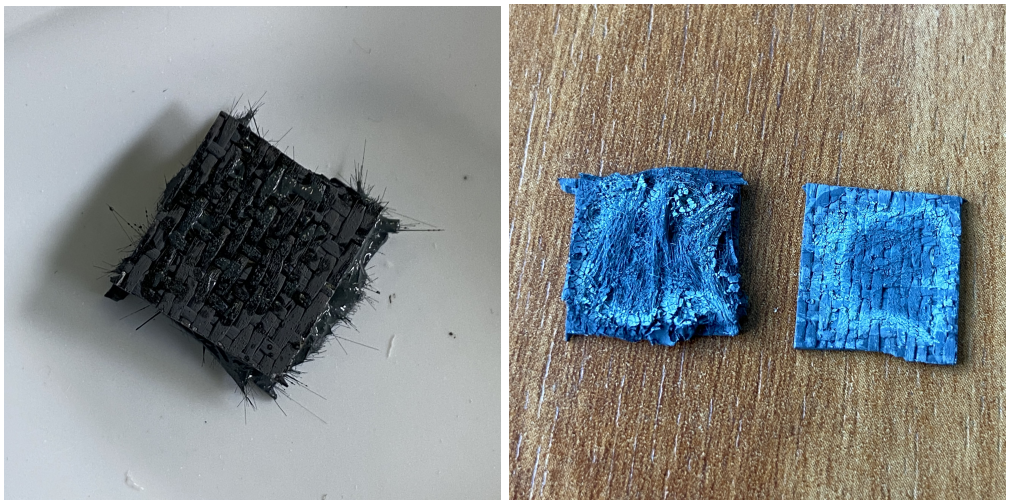

(a) Before process (b) After process

Figure 4.11: Sample TT4

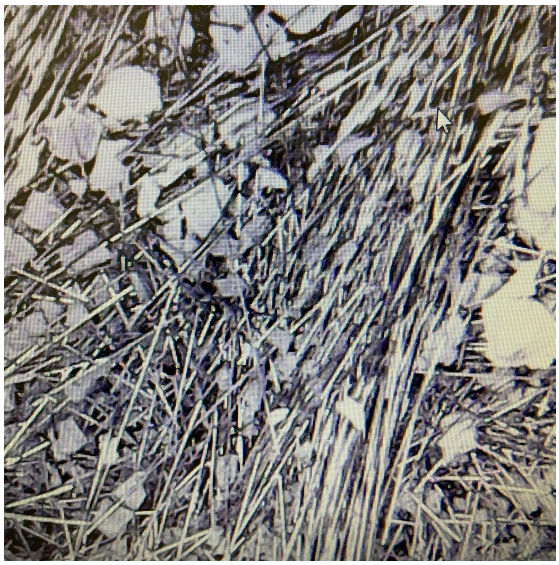

Figure 4.12: Optical microscopy of TT4 surface after pyrolysis

In conclusion, TT4 was important to have an idea of the upper limit of the fibers percentage and to understand that the mixing process must be longer and more accurate with respect to the experiments with the powder as filler.

The next substrates joining (from TT5 to TT7) were successful tests, achieved with a mixture of Tethon 3D and fibers respectively with mass contribution of 98.7% and 1.3% before the thermal process. The joints are shown in figure 4.13 in the crucible right after sintering and pyrolysis. After the pyrolysis, the samples were solidly joined, together with TT8 (the first tube-cap joining attempt).

Particularly, TT5 was a re-infiltration of the TT4 joining, that was done because the joint broke afterwards (so it was very simple to re-infiltrate) and only one of the two faces did not perform and adhesive behavior, that means that the other face had a good wettability, and the work had to be executed exclusively on the right face in figure 4.11b. In figure 4.13, TT5 is the upper-left one.

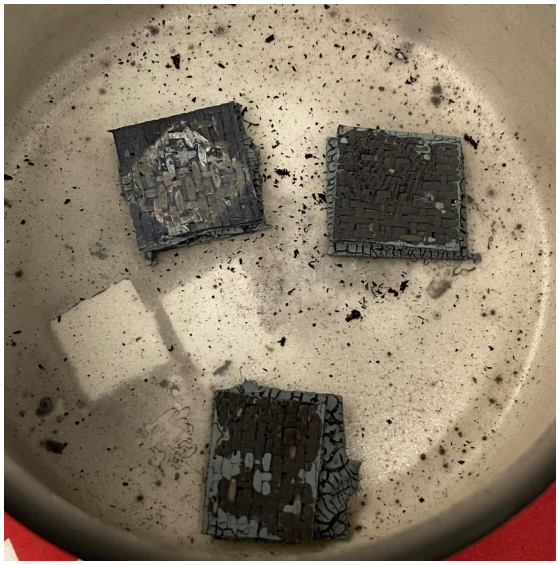

Figure 4.13: TT5-TT7 after process

The final Tethon slab joining, designated TT15, was created using SiC/SiC scraps and followed the process outlined in the previous section, which involved an extended curing period at a higher temperature. Additionally, the slurry amount was increased to produce a thicker joining region. After curing, the sample reached a solid state with a high concentration of fibers integrated into the matrix, as shown in figure 4.14a.

In figure 4.14b it is shown the sample after the pyrolysis process. The joining material exposed shows a good cohesion and adhesion to the bigger substrate.

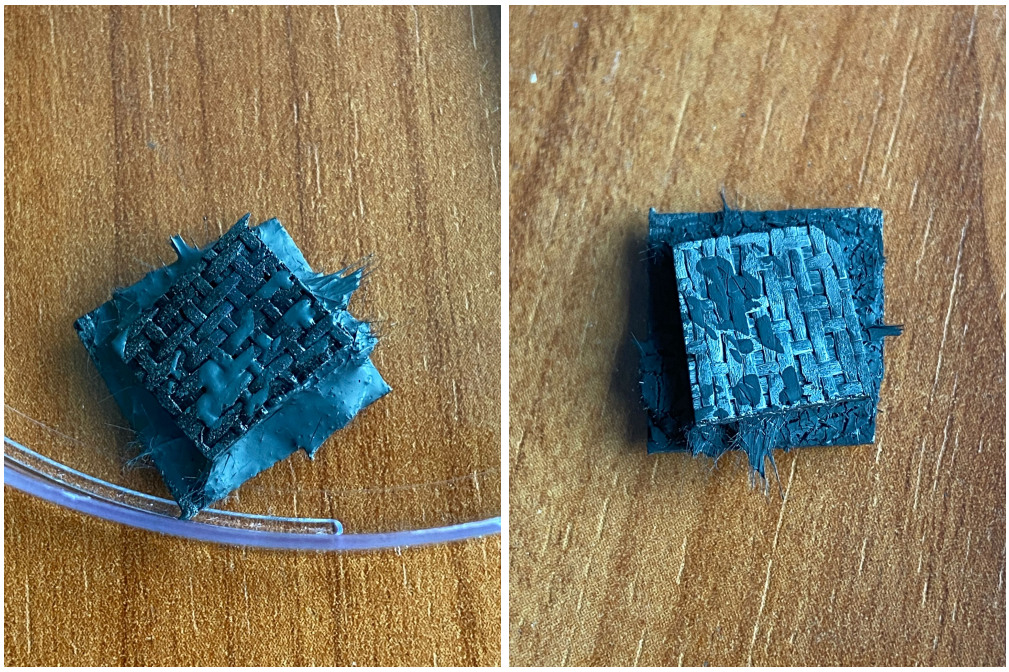

(a) After curing (b) After pyrolysis

Figure 4.14: TT15

4.3 Tube-cap joining

The tube-cap joining activity represents the final step of this thesis and it is aimed to obtain the mechanical joint between a cylinder and a cap with dimensions comparable in thickness to the nuclear fuel claddings in current LWRs. The cylinder has an internal diameter of 8 mm and a thickness of 1 µm, while it is long 50 mm, value that, on the other hand, is far from the real length of a fuel cladding (of about 4 m). It is supplied by CEA and composed of SiC_f/SiC, as in figure 4.15.

The change of joining geometry added a number of complications to the process: the joining area is not flat anymore, so the plasma cleaning is not trivial to apply because of the thinner and circular edge of the cylinder and of the cap. Also, the homogeneity of the application of the polymer mixture is not so simple and overall is not stable because it is affected by the force of gravity, while in a flat joining that is not a problem.

(a) (b)

Figure 4.15: Tube-cap system to be joined

Figure 4.16: Application of the polymer

The slurry was applied on the whole internal lateral surface of the cap and on the two thin connecting layers, in the tube and in the cap. During the entire process it has been attempted to maintain the sample as vertical as possible to guarantee a wetting as uniform as possible in the axial joining surfaces. Successful tube-cap joints have been tested also mechanically with the machine described in the previous chapter.

An efficient cleaning with plasma etching has been achieved by applying the procedure on all the three surfaces the slurry has been applied to, but through a grip the samples have been moved during the treatment to guarantee an uniform distribution of the plasma.

The first tube-cap test, named TT8, was achieved with a mixture of Tethon polymer and Hi-Nicalon type-S fibers, with respectively mass percentages 98.7% and 1.3%. After the curing step the polymer did not look cross-linked, but the sample post-pyrolysis showed a successful attachment, so it was decided to do a mechanical test. The results of it showed a maximum stress of a few Newton, low values with respect to the objective of the activity.

Nevertheless, after the rupture, the joining surfaces showed a very good adhesion with the polymer, as showed in figure 4.17. This means that the improvement is to be researched in the cohesion rather than in the adhesion.

The experiment TT9 showed in figure 4.18, with a fibers mass percentage of 4.1%, gave similar results, except for an evident heavier presence of fibers. The mixture for TT9 was the same used for the coating TT10, in figure 4.3, that gave good adhesion results.

(a) Cap (b) Tube

Figure 4.17: TT8

(a) Cap (b) Tube

Figure 4.18: TT9

The mechanical tests were the first ones ever done on this joints, and so it has been decided to test also those from the master thesis of De Angelis [35]. This latter gave a stress peak of 5 N, that compared to the other tests is a low value; this difference is due to a lower quantity of slurry applied, especially in the interstitial gap in the penetration zone. The broken sample after the mechanical fracture presented some pyrolyzed SiC in the external area, but almost none in the internal cylindrical surface, while samples TT8 and TT9 showed good adhesion even in that area, that it helped the joints to be more resistant.

TT8's cap was analyzed at SEM, giving the results in figures 4.19 and 4.20. Particularly, figure 4.19 contains details on the cap's groove, while figure 4.20 is a snapshot of the lateral surface of the cap.

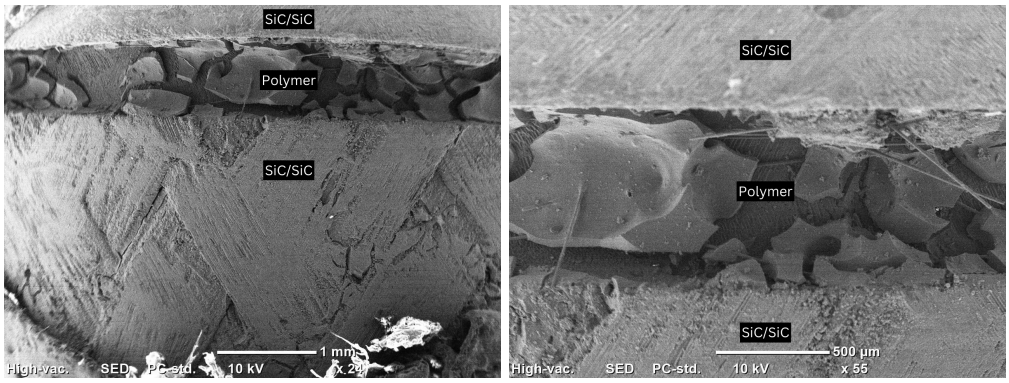

(a) (b)

Figure 4.19: TT8's cap SEM analysis (upper part)

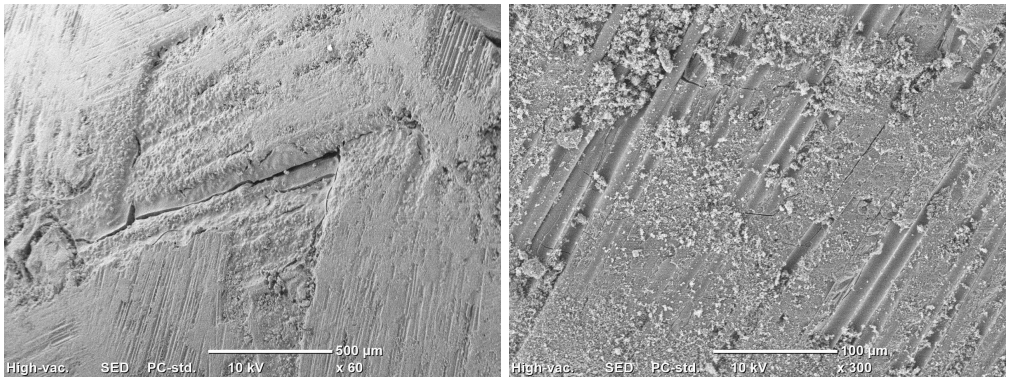

(a) (b)

Figure 4.20: TT8's cap SEM analysis (lateral surface)

It is noticeable that in the cap's upper part, the polymer pyrolyzed in clusters, similarly to the coating of pure Theton in figure 4.2. Figure 4.19b, that is a higher magnification of 4.19a, illustrates that the fibers enhance material cohesion by linking and consolidating the clusters. This means that the same sample with a higher percentage of fibers would have probably given better results.

The surface analysis, on the other hand, shows a much more compact output, probably given by the higher pressure between the two walls (the cap's external and the tube's internal), which are very close to each other. The next samples were treated with a weight on the top of the system to guarantee a better adhesion even in the upper part.

The sample TT9 was re-infiltrated by repeating the process and by applying it on the surface already treated. The experiment is called TT11, and for this it was used the same mixture of fibers and powder in the slurry described in table 4.2 applied to the the case TT12. The macroscopical result of the experiment is shown in figure 4.21.

Figure 4.21: TT11

The re-infiltration gave a satisfactory result about the adhesion of the polymer to the lateral surfaces, but it is evident in the microscopy in figure 4.22, done before the mechanical test, that the joining occurred only in the vertical cylindrical surfaces, while in the gap between the tube and the cap the adhesion is reduced or inexistent, because there are just a few pieces of SiC matrix that cross the whole gap and wet both the lower and the upper part.

Figure 4.22b shows a more promising region of the joint compared to figure 4.22a, primarily due to a higher concentration of fibers. However, it is important to note that this represents only a localized area, as the majority of the joint resembles the structure seen in Figure 4.22a, where there is visible separation from the cap. Furthermore, even in this improved region, there is still a significant presence of cracks. Overall, the joint's structural integrity appears to rely primarily on the lateral area rather than the gap area. This presents a challenge, as it means the joint may exhibit good torsional strength but is likely to be much more vulnerable to tensile stress, which is, in fact, the type of mechanical test conducted.

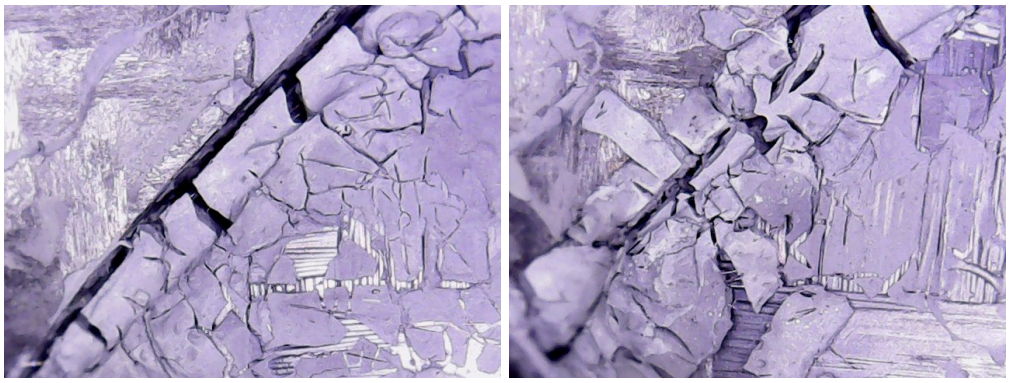

(a) (b)

Figure 4.22: Microscopy of the TT11 external joining area

The sample TT11 was mechanically tested and as expected the output was not a satisfactory stress-strain graph, because the peak stress had a value of barely 10 N.

In the subsequent tube-cap experiment, TT13, the same slurry and, most importantly, the same curing procedures as used in the coating sample TT14 were applied. Like TT14, TT13 demonstrated effective polymer cross-linking, with strong adhesion and solidification after the curing process in the oven, which was conducted at 200°C for a total of 2 hours.

The aspect is compact and without cracks because the material, even if cross-linked, was still a polymer. In addition, the amount of fibers in the groove was decisively increased in order to avoid the void effect obtained with the sample TT11 (figure 4.22).

The outcome of the new curing process is shown in figure 4.23, which also highlights the increased fiber density in the groove. The layer thickness in this area is enhanced due to the application of a steel weight over the cap during the oven curing process.

Figure 4.23: TT13 after curing

Figure 4.24: Macroscopy of TT13 after pyrolysis

The thermal process continued in the Xerion oven in inert atmosphere with a tungsten weight on the cap. The enhancements in the process made the sample be more cohesive in the groove region and overall to have a direct material connection between the tube and the cap even in that region.

What it is noticeable in the result, shown in figure 4.24, is that the joining material has cracks, that is expected because it was a new sample, meaning that no re-infiltration were done yet, but it is present both in the tube and in the cap.

A microscopy image of the joining region in sample TT13 is presented in figure 4.25. The figure highlights the quantity and uniform distribution of fibers within the groove area, where the matrix exhibits strong cohesion and good adhesion to the fibers. The image also illustrates the substantial impact of fiber presence on cohesion; in the upper and lower areas outside the groove, where fiber density is lower, the polymer matrix appears more fragmented.

The mechanical tests on this sample presented a maximum stress of around 15 N. It must be pointed out that all the obtained values are low

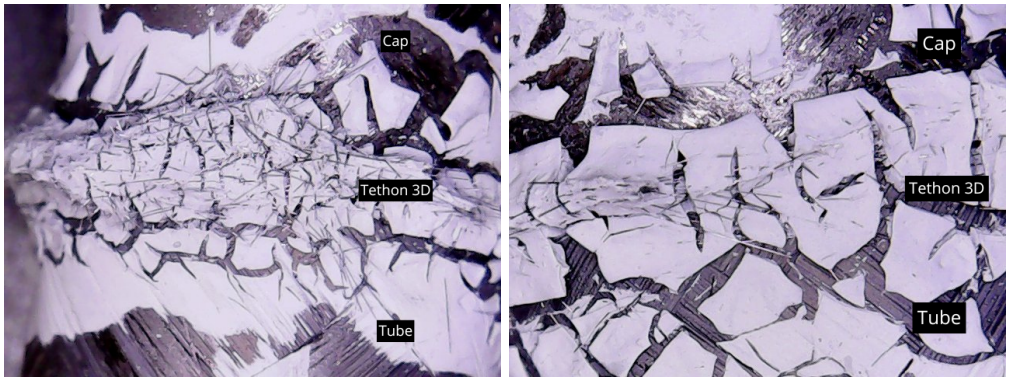

(a) (b)

Figure 4.25: Microscopy of TT13

with respect to the aim of the activity, but they represent a good starting point to improve.

The stress-strain graph of the last samples is shown in figure 4.26, where TT13 is the green one. It shows a good plastic deformation before fracture, and that is given by the presence of fiber bundles, as it has been noted in figure 4.27, where a bundle remained attached to the tube and to the cap.

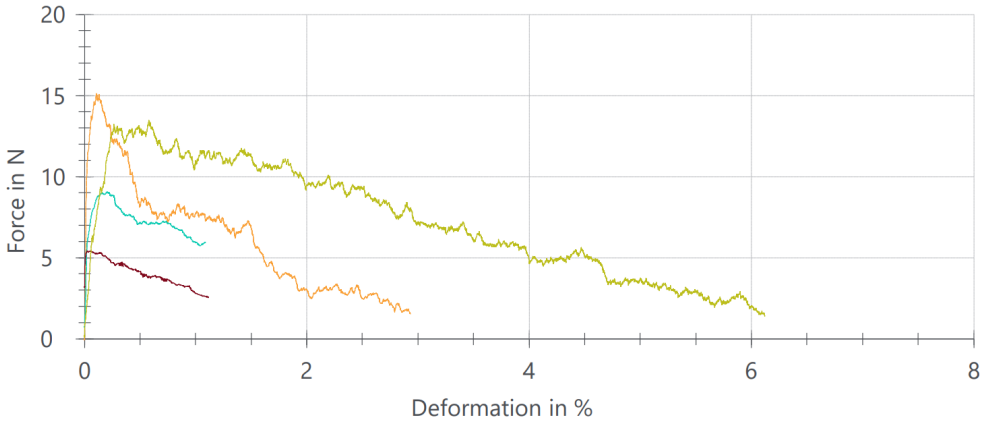

Figure 4.26: Stress-strain graphic

In figure 4.27 it is also clear that the joining material infiltrated homogeneously inside of the gap between the tube and the cap and contributed to the cohesion and airtightness of the joint.

The TT13 sample represents the last tube-cap joint accomplished using the slurry supplied by Tethon 3D in this thesis work.

(a) Tube (b) Cap

Figure 4.27: Fiber bundles attached to the sample after mechanical test - TT13

Chapter 5

Conclusion and discussion

This thesis work is part of the European project "Scorpion", aimed to find alternative materials and industrial techniques in order to substitute the current main technology in the nuclear fuel claddings in LWRs, Zr-based alloys, that present noticeable disadvantages with respect to the potential of other materials.

The used material is SiC_f/SiC. The challenge in this project was to join a tube-cap system, that is meant to seal the cladding, with a pre-ceramic polymer in order to obtain a joint composed by the same material, in this case silicon carbide. The polymer mostly used was supplied by the American company Tethon 3D and it was liquid, but in the final period of the work another polycarbosilane in a solid state supplied by WORLDEX Industry & Trading Co. was tested.

Through the use of the tools and machines from the DISAT laboratory, coating, substrates and finally tube-cap joinings were made and then analyzed with advanced analysis tools such as CT-scan; successively, the most significant ones were mechanically tested and characterized.

Update meetings and technical discussion aimed to improve the results were done weekly with the team and the used techniques changed during the activity due to refining, discoveries and change of materials, including the filler, going from powder to fibers, and the matrix, changing the supplier of polycarbosilane from fluid to solid. Important factors manipulated in progress were the precision in the plasma etching process to improve the surface wettability, the percentage and the type of added fibers, the pressure between the substrates during the thermal treatment, the quantity of slurry applied and the specifics of the cross-linking step (temperature and duration).

After the adjustment of the various parameters, it was achieved to obtain planar joints with 1.5x1.5cm^2 substrates. Successively, it was possible to apply the mixtures with the same characteristics to the tube-cap geometry. Since the first attempts, the cylindrical joints showed a very good adhesion to the surface and integrity, but the internal cohesion was rather weak, as the mechanical tests demonstrated.

The cohesion was then improved with a higher percentage of SiC Hi-Nicalon type-S fibers, but the tensile stress resistance is still far from the results obtained with other technologies such as SAY glass-ceramic or laser joining.

Specifically concerning the tube-cap joint, that was the main purpose of the thesis, the improvements in the state of art of the activity have been:

- Carrying out mechanical tests on the previous and new experiments
- Using various types of fillers, specifically ground powder of SiC/SiC, and SiC Hi-Nicalon type-S fibers
- Realizing re-infiltrations on the samples to enhance the cohesion in the joining area
- Realizing an extended plasma treatment to prepare the surfaces

To sum up, the experiments with the Tethon slurry resulted in a series of joints, where the optimal amount of added fibers was determined through trial and error. However, a more precise evaluation could be achieved through a scientific approach, utilizing the underlying physics of the process.

The future implications of this thesis relate to both material selection and process optimization. Although the joining process developed with the Tethon 3D polymer shows promise, it remains imperfect and can be further refined, particularly by determining the optimal matrix-to-filler ratio through methods beyond trial and error. Additionally, the material explored in this work is just one polycarbosilane option among many, such as the solid polycarbosilane offered by WORLDEX Industry & Trading Co. Testing alternative polycarbosilanes, following discussions with suppliers, may reveal materials better suited to enhancing joint performance.

The distribution of the fibers is a topic to be deepen as well: the fibers can be tailored and applied in different ways. For instance, longer fibers can be added on the external region after the slurry is applied, to enhance the connection between the tube and the cap.

Bibliography

[1] Structure and properties of ceramics. *The American Ceramic Society*.

[2] Jan Coenen. Fusion materials development at forschungszentrum jülich. *Advanced Engineering Materials*, 22, 04 2020.

[3] Jiaming Bai. Additive manufacturing of ceramics: Materials, characterization and applications. 2023.

[4] Alessandro De Zanet. Plasma etching as a surface engineering technique for sic/sic composites to improve joint strength. *Ceramics International*, 2023.

[5] M Altahhan. Multiphysic analysis of cmc silicon carbide and zircaloy cladding. 2018.

[6] Nikola Jak˘si´c. Nuclear fuel cladding review of the zircaloy cladding and basic analysis of the model with the single hydride dg jrc institute for energy. *Institute for Energy*, 2008.

[7] WEON-JU KIM, DAEJONG KIM, and JI YEON PARK. Fabrication and material issues for the application of sic composites to lwr fuel cladding. *Nuclear Engineering and Technology*, 45(4):565–572, 2013.

[8] A.R Raffray, R Jones, G Aiello, M Billone, L Giancarli, H Golfier, A Hasegawa, Y Katoh, A Kohyama, S Nishio, B Riccardi, and M.S Tillack. Design and material issues for high performance sicf/sic-based fusion power cores. *Fusion Engineering and Design*, 55(1):55–95, 2001.

[9] George Newsome, Lance L. Snead, Tatsuya Hinoki, Yutai Katoh, and Dominic Peters. Evaluation of neutron irradiated silicon carbide and silicon carbide composites. *Journal of Nuclear Materials*, 371(1):76–89, 2007. Nuclear Fuels and Structural Materials 1.

[10] Alex G. Perez-Bergquist, Takashi Nozawa, Chunghao Phillip Shih, Keith J. Leonard, Lance Lewis Snead, and Yutai Katoh. High dose neutron irradiations of hi-nicalon type s silicon carbide composites, part 1: Microstructural evaluations. *Journal of Nuclear Materials*, 462(7), 7 2014.

[11] Vera Haase, Gerhard Kirschstein, Hildegard List, Sigrid Ruprecht, Raymond Sangster, Friedrich Schröder, Wolfgang Töpper, Hans Vanecek, Werner Heit, Jürgen Schlichting, and Hartmut Katscher. *The Si-C Phase Diagram*. Springer Berlin Heidelberg, 1985.

[12] M. Ferraris, M. Salvo, C. Isola, M. Appendino Montorsi, and A. Kohyama. Glass-ceramic joining and coating of sic/sic for fusion applications. *Journal of Nuclear Materials*, 258-263:1546–1550, 1998.

[13] V Chaumat. *Brazing of SiC materials for space applications*. 2017.

[14] S. Hausner and B. Wielage. 12 - brazing of metal and ceramic joints. In Dušan P. Sekulić, editor, *Advances in Brazing*, Woodhead Publishing Series in Welding and Other Joining Technologies, pages 361–393. Woodhead Publishing, 2013.

[15] M De Vivo. Giunzioni di compositi sicf/sic per applicazioni nel settore dell'energia nucleare. Master's thesis, Politecnico di Torino, 2021.

[16] Bofang Zhou, Jinfeng Wang, Keqin Feng, Yuchen Cai, and Sitan Chen. Effect of brazing parameters on the microstructure and properties of sic ceramic joint with zr-cu filler metal. *Crystals*, 10:93, 02 2020.

[17] Yutai Katoh, Lance L. Snead, Ting Cheng, Chunghao Shih, W. Daniel Lewis, Takaaki Koyanagi, Tatsuya Hinoki, Charles H. Henager, and Monica Ferraris. Radiation-tolerant joining technologies for silicon carbide ceramics and composites. *Journal of Nuclear Materials*, 448(1):497–511, 2014.

[18] Miladin Radovic and Michel W. Barsoum. Max phases: Bridging the gap between metals and ceramics. *American Ceramic Society Bulletin*, 92(3):20 – 27, 2013.

[19] Per Eklund, Johanna Rosen, and Per O Å Persson. Layered ternary mn+1axn phases and their 2d derivative mxene: an overview from a thin-film perspective. *Journal of Physics D: Applied Physics*, 50(11):113001, feb 2017.

[20] Matheus A. Tunes, Sean M. Drewry, Jose D. Arregui-Mena, Sezer Picak, Graeme Greaves, Luigi B. Cattini, Stefan Pogatscher, James A. Valdez, Saryu Fensin, Osman El-Atwani, Stephen E. Donnelly, Tarik A. Saleh, and Philip D. Edmondson. Accelerated radiation tolerance testing of ti-based max phases. *Materials Today Energy*, 30:101186, 2022.

[21] Takaaki Koyanagi, Yutai Katoh, Kurt A. Terrani, Young-Jin Kim, James O. Kiggans, and Tatsuya Hinoki. Hydrothermal corrosion of silicon carbide joints without radiation. *Journal of Nuclear Materials*, 481:226–233, 2016.

[22] Yutai Katoh, M Kotani, A Kohyama, M Montorsi, M Salvo, and M Ferraris. Microstructure and mechanical properties of low-activation glass-ceramic joining and coating for sic/sic composites. *Journal of Nuclear Materials*, 283-287:1262–1266, 2000. 9th Int. Conf. on Fusion Reactor Materials.

[23] M. Ferraris, V. Casalegno, S. Rizzo, M. Salvo, T.O. Van Staveren, and J. Matejicek. Effects of neutron irradiation on glass ceramics as pressure-less joining materials for sic based components for nuclear applications. *Journal of Nuclear Materials*, 429(1):166–172, 2012.

[24] Takaaki Koyanagi, Yutai Katoh, Tatsuya Hinoki, Charles Henager, Monica Ferraris, and Salvatore Grasso. Progress in development of sic-based joints resistant to neutron irradiation. *Journal of the European Ceramic Society*, 40(4):1023–1034, 2020.

[25] Masao Tokita. Progress of spark plasma sintering (sps) method, systems, ceramics applications and industrialization. *Ceramics*, 4(2):160–198, 2021.

[26] Zhang Bo, Zhang Lixia, Pan Hui, Sun Zhan, and Chang Qing. Low-temperature diffusion bonding of ti3si(al)c2 ceramic with au interlayer. *Journal of the European Ceramic Society*, 42(8):3415–3426, 2022.

[27] Salvatore Grasso, Valentina Casalegno, and Monica Ferraris. Flash joining of cvd-sic coated cf/sic composites with a ti interlayer. 2017.

[28] Pardeep Kumar Gianchandani, Valentina Casalegno, Milena Salvo, Monica Ferraris, and Ivo Dlouhý. "refractory metal, rm – wrap": A tailorable, pressure-less joining technology. *Ceramics international*, 45(4):4824–4834, 2019.

[29] Current status of materials development of nuclear fuel cladding tubes for light water reactors. *Nuclear engineering and design*, 316:131–150, 2017.

[30] S. Suyama, T. Kameda, and Y. Itoh. Development of high-strength reaction-sintered silicon carbide. *Diamond and Related Materials*, 12(3):1201–1204, 2003. 13th European Conference on Diamond, Diamond-Like Materials, Carbon Nanotubes, Nitrides and Silicon Carbide.

[31] Gilvan Barroso, Quan Li, Rajendra K. Bordia, and Günter Motz. Polymeric and ceramic silicon-based coatings – a review. *J. Mater. Chem. A*, 7:1936–1963, 2019.

[32] Dong-Hyuk Jeong, Arifin Septiadi, Pipit Fitriani, and Dang-Hyok Yoon. Joining of sicf/sic using polycarbosilane and polysilazane preceramic mixtures. *Ceramics International*, 44(9):10443–10450, 2018.

[33] Paolo Colombo, Gabriela Mera, Ralf Riedel, and Gian Domenico Sorarù. Polymer-derived ceramics: 40 years of research and innovation in advanced ceramics. *Journal of the American Ceramic Society*, 93(7):1805–1837, 2010.

[34] Raghvendra Pratap Chaudhary, Chithra Parameswaran, Muhammad Idrees, Abolaji Sefiu Rasaki, Changyong Liu, Zhangwei Chen, and Paolo Colombo. Additive manufacturing of polymer-derived ceramics: Materials, technologies, properties and potential applications. *Progress in Materials Science*, 128, 2022.

[35] S De Angelis. Processi di giunzione per compositi a base di carburo di silicio. Master's thesis, Politecnico di Torino, 2024.

[36] Peter Greil. Active-filler-controlled pyrolysis of preceramic polymers. *Journal of the American Ceramic Society*, 78(4):835–848, 1995.

[37] Raghvendra Pratap Chaudhary, Chithra Parameswaran, Muhammad Idrees, Abolaji Sefiu Rasaki, Changyong Liu, Zhangwei Chen, and Paolo Colombo. Additive manufacturing of polymer-derived ceramics: Materials, technologies, properties and potential applications. *Progress in Materials Science*, 128:100969, 2022.

[38] *Tethon 3D.*

[39] Heshan Ezzat Khalifa. High durability joints between ceramic articles, and methods of making and using same. *United States Patent No. US 9,132,619 B2*, 2015.

[40] Peter Greil. Active-filler-controlled pyrolysis of preceramic polymers. *Journal of the American Ceramic Society*, 78(4):835–848, 1995.

[41] Vipin Vijay, V.M. Biju, and Renjith Devasia. Active filler controlled polymer pyrolysis – a promising route for the fabrication of advanced ceramics. *Ceramics international*, 42(14):15592–15596, 2016.

[42] Nilda Martins. Development of plasma assisted pyrolysis of polymer derived ceramic coatings on sintered steel. 2017.

[43] Virginia Pastorelli. Preparation and characterization of joints with preceramic polymers with the aim of energy efficiency and saving. Master's thesis, Politecnico di Torino, 2023.

[44] Yutai Katoh and Lance L. Snead. Silicon carbide and its composites for nuclear applications – historical overview. *Journal of Nuclear Materials*, 526:151849, 2019.

[45] *DISAT PoliTo http://www.composites.polito.it/?p=people.*

[46] F.J. Fuchs. 19 - ultrasonic cleaning and washing of surfaces. In Juan A. Gallego-Juárez and Karl F. Graff, editors, *Power Ultrasonics*, pages 577–609. Woodhead Publishing, Oxford, 2015.

[47] Alessandro De Zanet. Atmospheric pressure plasma jet for surface texturing of c/sic. *Ceramics International*, 2023.

[48] Plasmatec-x - atmospheric plasma: product information.

[49] Peng Xiao, Zhuan Li, Zibing Zhu, and Xiang Xiong. Preparation, properties and application of c/c-sic composites fabricated by warm compacted-in situ reaction. *Journal of Materials Science & Technology*, 26(3):283–288, 2010.

[50] polito.it. Fornace sottovuoto xvac. *Politecnico di Torino.*

[51] Freundchen. Schematische darstellung des birnenförmigen anregungsbereiches bei der rasterelektronenmikroskopie und veranschaulichung der unterschiedlichen emissionstiefen für detektierbare teilchen und strahlung. 2012.

[52] Dale E. Newbury and Nicholas W. M. Ritchie. Is scanning electron microscopy/energy dispersive x-ray spectrometry (sem/eds) quantitative? *Scanning*, 35(3):141–168, 2013.